Published in final edited form as:
Biochim Biophys Acta. 2013 ; 1827(0): 1295–1308. doi:10.1016/j.bbabio.2013.03.002.

Transmembrane Signaling and Assembly of the Cytochrome b_6f-Lipidic Charge Transfer Complex

S. Saif Hasan[1], **E. Yamashita**[2], and **William A. Cramer**[1,*]

[1]Department of Biological Sciences, Purdue University, West Lafayette, IN 47907, USA

[2]Osaka University, Institute for Protein Research, Suita, Osaka 565-0871, Japan

Abstract

Structure-function properties of the cytochrome b_6f complex are sufficiently unique compared to those of the cytochrome bc_1 complex that b_6f should not be considered a trivially modified bc_1 complex. A unique property of the dimeric b_6f complex is its involvement in trans-membrane signaling associated with the p-side oxidation of plastoquinol. Structure analysis of lipid binding sites in the cyanobacterial b_6f complex prepared by hydrophobic chromatography shows that the space occupied by the H transmembrane helix in the cytochrome *b* subunit of the bc_1 complex is mostly filled by a lipid in the b_6f crystal structure. It is suggested that this space can be filled by the domain of a transmembrane signaling protein.

The identification of lipid sites and likely function define the intra-membrane conserved central core of the b_6f complex, consisting of the seven trans-membrane helices of the cytochrome *b* and subunit IV polypeptides. The other six TM helices, contributed by cytochrome *f*, the iron-sulfur protein, and the four peripheral single span subunits, define a peripheral less conserved domain of the complex.

The distribution of conserved and non-conserved domains of each monomer of the complex, and the position and inferred function of a number of the lipids, suggests a model for the sequential assembly in the membrane of the eight subunits of the b_6f complex, in which the assembly is initiated by formation of the cytochrome b_6-subunit IV core sub-complex in a monomer unit. Two conformations of the unique lipidic chlorophyll *a*, defined in crystal structures, are described, and functions of the outlying β-carotene, a possible 'latch' in supercomplex formation, are discussed.

Introduction

. Oxygenic photosynthesis is responsible for conversion of light energy from the sun into chemical energy stored in sugars and ATP [1]. The primary photosynthetic reactions utilizing solar energy involve the oxidation of water by the Photosystem II (PSII) protein

*waclab@purdue.edu, phone: 765-494-4956, fax: 765-496-1189.

complex to release molecular oxygen, electrons and protons (**Fig. 1**). On the reducing side of PSII, lipophilic plastoquinone (PQ) is reduced to plastoquinol (PQH_2), which diffuses laterally in the membrane to the cytochrome b_6f complex (cyt b_6f). The protons released by hydrolysis of H_2O contribute to the transmembrane proton electrochemical gradient, $\Delta\tilde{\mu}H+$. The b_6f complex catalyzes PQH_2deprotonationand oxidation on the lumen (electrochemically positive, p) side of the thylakoid membrane, and PQ reduction and protonation on the stromal (electrochemically negative, n) side. p-side PQH_2 is oxidized by a series of sequential one electron carriers in the high potential electron transport chain consisting of: (i) the membrane bound [$2Fe_2$-2S] cluster in the iron-sulfur protein (ISP), usually in coordination with the p-side heme b_p of the cyt b_6 subunit of the complex, (ii) the cytochrome *f* heme in the p-side peripheral domain, (iii) soluble plastocyanin (PC) or cyt c_6, and (iv) the photosystem I (PSI) reaction center.

Structure of the cyt b_6f complex

The cyt b_6f complex is a symmetric dimer [2, 3] [4] (**Fig. 2A, B**) that consists of eight trans-membrane polypeptide subunits. The b_6f monomer has two polytopic subunits, cytochrome b_6 (cyt b_6) and subunit IV (subIV). Cyt b_6 (~25 kDa, encoded by *petB*) consists of a four-transmembrane helix (TMH) bundle and a short soluble helix formed by the N-terminal 28-29 amino acids, which is associated with the n-side membrane surface. TMH helices are labeled A-D. The four TMH of cytb_6 are connected by loops that are located at the p and n-side membrane-water interfaces. SubIV (~17 kDa, encoded by *petD*) has three TMH (E-F) that form a p-side saddle around the four helix bundle of cyt b_6. Helix E is located in proximity to the A and B-helix of cyt b_6 while the F and G-TMHs span the four helix bundle, close to the B and C-TMH (**Fig. 2C**). The C-terminus of the E-TMH is separated from the N-terminus of the F-TMH by a distance of ~40 Å, which is bridged by the p-side *ef*-loop. This seven TMH assembly forms the polytopic core of the cyt b_6f complex. Six single TMH arising from individual subunits are arranged in the periphery around the core of the monomeric unit of the complex consisting of the cyt b_6-subIV subunits: (**i**) cytochrome *f* (cyt *f*, ~32 kDa, encoded by *petA*) and**(ii**) the Rieske Iron-Sulfur Protein (ISP, ~19 kDa, *petC*) each contain a large soluble domain on the p-side, attached to one TMH and, (**iii-vi**) four small (3-4 kDa) subunits, Pet G (gene *petG*), L (gene *petL*), M (gene *petM*) and N (gene *petN*), define a four-helix bundle on the periphery of each monomer of the complex, on the peripheral side opposite the inter-monomer cavity (**Fig. 2D**).

Prosthetic groups

The cyt b_6f monomer has seven prosthetic groups [2, 3, 5] (**Fig. 2A, B**). Within the trans-membrane region, the B and D TMHs of cyt b_6 are associated with two bis-histidine ligated *b*-hemes (b_p and b_n, on the p and n-side). The conserved His86/His187of the B and D TMH provide axial coordination to heme b_p while His100/His202 of the B and D TMH coordinate heme b_n [2, 3, 6]. A unique covalently linked heme c_n is found to be electronically coupled to heme b_n through an axial H_2O or OH^- ion, on the n-side of the complex [2, 3, 7, 8] (**Figs. 2A, 3**). In the absence of a second axial ligand, heme c_n is a high spin heme, with a small extinction coefficient in the visible range [9]. Cys35, a conserved residue that is found not only in the photosynthetic cyt b_6 polypeptide but also in the cyt *b* protein of non-

photosynthetic firmicutes [10], forms a covalent thioether linkage to heme c_n (**Fig. 2C**). A chlorophyll-*a* (chl-*a*) and a β-carotene (β-car) molecule are also inserted between the hydrophobic TMHs (**Fig. 2B**). In the p-side peripheral domain, the cyt *f* polypeptide is covalently linked to a heme molecule (a *c*-type heme) while the ISP extrinsic domain binds one [2Fe-2S] cluster. The midpoint redox potentials at pH 7 of the prosthetic groups involved in electron transfer are summarized in **Table 1**.

The inter-monomer cavity

The dimeric structure of cyt b_6f is organized around an inter-monomer cavity (30 Å high × 25 Å wide × 15 Å deep) [2, 3, 5] (**Figs. 2A, B**). On the n-side, the cavity is marked by the N-terminal soluble helix of cyt b_6 and on the p-side by residues from the A and D-TMH of cyt b_6. Within the lipid bilayer, the interior of the cavity is lined by amino acids from the A and D-TMH of cyt b_6, the E-helix of subIV and the ISP TMH. The cavity is considered to provide the space that sequesters the substrate PQH_2 from the membrane bilayer generated by PSII and thus to concentrate the quinol near the p-side oxidation (Q_p) site in the complex [11]. The structure around the inter-monomer cavity is stabilized through interactions between residues of cyt b_6 and subIV within the trans-membrane region. The Rieske ISP TMH is associated with the cyt *f* TMH of one monomer while its soluble domain crosses-over to the other monomer (**Fig. 2A**), where it interacts with the p-side soluble domain of cyt *f* and the trans-membrane regions of cyt b_6 and subIV. Further stabilization of the dimeric structure is provided by lipid molecules [12] (**Fig. 2B**) (and see below).

Crystal structures of the cyt b_6f complex have been obtained from the prokaryotic filamentous cyanobacteria *Nostoc* PCC 7120[5], *M. laminosus* [2] [13], and the eukaryotic green alga *Chlamydomonas reinhardtii* [3]. Structures of the ~250 residue cyt *f* peripheral domain have been obtained from *C. reinhardtii* [14, 15], *Phormidium laminosum* [16], *Brassica rapa* [17-19], while those of the ISP soluble domain have been solved from tryptic fragments of the ISP protein isolated from *Thermosynechococcus elongates* [20] and *Spinacia olearcea* [21]. While the trans-membrane region of the b_6f complex consists of α-helices, the N-terminal soluble domain of cyt *f* has an elongate β— sheet structure (**Fig. 2A**). The covalently linked heme *f* is located in the peripheral subdomain proximal to the cyt *f* TMH via an unusual ligation of the Tyr1 side chain to the heme Fe, along with an imidazole axial linkage from the side chain of His26 [22]. The entire cyt *f* soluble domain extends as an elongate 75 Å bowl shaped structure within which the ISP soluble domain is encompassed. The ISP C-terminal soluble domain is attached to the TMH through a poly-glycine hinge region [2, 3, 5] (**Fig. 2A**), which gives the soluble domain flexibility for motion crucial to catalysis, and consists of β–sheets separated into two smaller domains. The redox active [2Fe-2S] cluster is linked to the subdomain extrinsic to the ISP TMH. His109 and His129 side chains coordinate the outer Fe atom of the cluster while the inner Fe is linked to Cys107 and Cys127.

Sequence and structure similarity between cyt b_6f and bc_1 complexes

Cyt b_6f and bc_1 constitute the family of cytochrome *bc* complexes [23]. Cyt b_6f and bc_1 share several structural features. The transmembrane quinol oxidoreductase and proton pumping function of cyt b_6f is performed by the homologous cyt bc_1 complex in

photosynthetic and denitrifying bacteria and in the membranes of mitochondria (**Fig. 4A**). Cyt b_6 has four TMH (**A-D**), as does the cyt *b* (bc_1) N-terminal domain. However, subIV has three TMH (E-G), one short of the four TMH found in the C-terminal domain of cyt *b*. The C-terminal 8th helix, labeled "H" in cyt *b* (bc_1), is absent from subIV. Structurally, the cyt b_6 subunit is arranged as the N-terminal domain four TMH of cyt *b*. SubIV has a slightly altered structure (**Fig. 4B**) due to insertion of the chl-*a* molecule between the F and G TMH, and the absence of helix H from subIV.

Sequence similarity between the single helix subunits of cyt b_6f and bc_1 is limited. The ISP subunit has a significant conservation of 47-61% in the sequence only in the cluster binding sub-domain [21, 24]. Structurally, the overall fold of the ISP soluble domain and TMH are very similar between b_6f and bc_1 except in the N-terminal region that constitutes the TMH on the n-side. In b_6f, the TMH of ISP is bent while that in the bc_1 complex forms a straight α-helix [3]. There is no conservation between the sequence and structure of the b_6f cyt *f* and the analogous cytochrome c_1 (cyt c_1) of bc_1. Both polypeptides provide a covalently linked heme that functions as the electron acceptor for the ISP [2Fe-2S] cluster, and hence, show convergent evolution. Structurally, cyt *f* consists of an elongated β-sheet extrinsic domain and one TMH, while the cyt c_1 soluble domain has a globular, α-helical arrangement (reviewed recently in [25]).

Function similarity between cyt b_6f and bc_1 complexes

Cyt b_6f and bc_1 complexes act as a plastoquinol:plastocyanin and ubiquinol:cytochrome *c* oxidoreductase, respectively, to catalyze a "*Q*-cycle" [26-32]. However, the mechanism of this cycle differs in the two complexes because of the presence of the heme c_n, possibly FNR, and of the PSI cyclic pathway in the b_6f complex [10]. The enzyme FNR, found in association with the b_6f complex on the n-side [33], may donate an electron from NADPH to the Q_n-site to complete the reduction of the plastoquinone, thereby decreasing the number of p-side PQH_2- oxidation events required for the n-side reduction of PQ. The association of b_6f with FNR may be an important evolutionary adaptation with significant kinetic consequences as the p-site quinol deprotonation reaction constitutes the rate limiting step in the activity of cyt *bc* complexes, with an activation energy of 32 kJ/mol [34, 35]. By providing an alternate route for electron delivery to the Q_n-site, FNR may contribute to acceleration of the rate of photosynthetic electron transfer.

Differences between cyt b_6f and bc_1 complexes

(**i**) In addition to the linear electron transport (LET) pathway, an additional pathway, the PSI cyclic pathway operates in oxygenic photosynthesis in a feedback mechanism to transfer electrons from the reducing n-side of PSI to the quinone pool via an n-side entry to cyt b_6f and/or complex I (**Fig. 1**), thereby balancing redox poise and regulating the ATP level needed for carbon fixation [10]. There is no corresponding pathway in the bc_1 complex. (**ii**) Heme c_n, which occupies much of the n-side quinone binding niche of the bc_1 complex, is electronically coupled to heme b_n from which it is separated by 4 Å [2, 3, 5]. (**iii**) The small Pet subunits of cyt b_6f, PetG, L, M and N, have no homologous substitutes in the bc_1 complex [2, 3]. Instead, their position is occupied by lipids in bc_1 [36]. (**iv**) Cyt bc_1 also has several extrinsic polypeptides, both soluble and transmembrane, that are found only in the

eukaryotic complex [37]. These subunits are absent in the prokaryotic bc_1 [38] and the photosynthetic b_6f complexes [2, 3]. (**v**) The b_6f complex contains three more prosthetic groups than bc_1. While both complexes have hemes b_p and b_n in the transmembrane region and a [2Fe-2S] cluster and a covalently linked heme in the soluble domains, the unique heme c_n, chl-*a* and β-car are not found in the bc_1 complex [39]. (**vi**) The architecture of the Q_p and Q_n sites also differs between the complexes due to the presence of a chl-*a* and the unique heme c_n in the b_6f complex. On the p-side, the heterocyclic chlorin ring of the chl-*a* molecule is located between the F and G TMH of subIV (**Fig. 2B**) while its long phytyl-tail passes into the portal of quinone entry that leads to the Q_p-site in b_6f [5, 11]. This portal is formed by residues from the C-helix of cyt b_6 and the F-helix of subIV and measures 12-15 Å in cross-section. The absence of chl-*a* from the bc_1 complex enlarges the Q_p-portal, which may have effects on the residence time of the substrate quinol within the Q_p-site, thereby providing a major difference between structure and kinetics on the p-side of cyt b_6f and bc_1. On the n-side, heme c_n (**Fig. 2C)** is located at the Q_n-site, with its open axial position facing the inter-monomer cavity. Crystallographic studies have implicated this open axial position as the quinone binding site in b_6f [13]. Compared to the Q_n-site of bc_1 that consists of an amino acid environment leading to heme b_n, the Q_n-site of b_6f provides greater access to the substrate quinone from the inter-monomer cavity. This structural difference has an important implication in reducing the selectivity and efficiency of inhibitor binding to the Q_n-site (discussed below), again providing for major structural, kinetic and equilibrium related differences between b_6f and bc_1. In summarizing the differences between the two sets of complexes, it can be said that the b_6f complex is not a trivially modified bc_1 complex.

Lipids associated with the b_6f complex

Membrane proteins depend on internal integral lipids for structural stability and biological activity [40-42]. The role of lipids in stabilizing the structure of membrane proteins, or even inducing structural changes within proteins has been investigated by methods that are sensitive to changes in secondary and tertiary structure, thermal stability assays using, for example, enzymatic activity, that provide information about the functional dependence of the protein on lipid content [40, 43].

It is now well documented that successful crystallization of a large number of membrane proteins depends on the presence of stabilizing lipids, as in the case of the photosynthetic light harvesting complex [44], bacteriorhodopsin [45], GPCRs [46] and aquaporin [47]. High resolution crystal structures of membrane proteins provided evidence for specific lipid-protein interactions, as deduced from the presence of well-defined lipid binding sites occupied by ordered lipids, both on the surface and within folded polypeptides. The class of membrane proteins that represents the largest number of well-defined lipid binding sites observed structurally is that of the hetero-oligomeric complexes that consist of distinct polypeptide subunits [48, 49]. Membrane protein complexes are assembled from protein components of different sizes and amino acid composition. The problem of packing the components together to form a stable membrane protein complex is solved by the incorporation of lipid molecules, which interact with the surrounding protein environment, mainly through Van der Waals interactions [50, 51]. Due to the non-specific nature of these interactions, it may be possible to substitute a natural lipid with a synthetic lipid without

affecting biological function [52-54]. During the process of purification, natural lipids may also be replaced by detergent molecules that serve as synthetic structural and functional analogs of lipids [48]. Due to the smaller volume occupied by a single tail, detergents tend to form micelles, and not bilayers like lipids [40]. The physico-chemical similarity between the properties of lipids and detergents has implications for the identification of lipid binding sites [48, 49]. The presence of a crystallographically well defined site with a bound detergent molecule is considered to mark the position of a natural lipid. Weakly bound lipids may be replaced by detergent molecules, especially at the surface of membrane proteins. Therefore, the analysis of lipid binding sites in membrane proteins is inclusive of sites occupied by natural lipids, synthetic lipids as well as ordered detergent molecules.

Prior to elucidation of the cyt b_6f crystal structure, a role of lipids in the structure had been inferred through biochemical studies [55, 56]. Successful crystallization of the cyanobacterial cyt b_6f complex to obtain highly diffracting crystals required the addition of a synthetic lipid to the purified and delipidatedb_6f preparation. Addition of the neutral lipid dioleoylphosphatidylcholine (DOPC) improved diffraction quality of b_6f crystals from 11 Å to 3 Å [2, 50]. Purification of the b_6f complex from the eukaryotic alga *C. reinhardtii* for successful crystallization was carried out under mild conditions of metal-affinity chromatography that did not remove lipids from the complex [3]. Elucidation of the structure of cyt b_6f from *C. reinhardtii* showed the presence of a total of 4 lipids and 4 detergent bound sites within the transmembrane domain, in addition to the hydrophobic photosynthetic pigments chl-*a* and β–carotene (**Fig. 2A, B**).

The use of hydrophobic chromatography allowed manipulation of lipid content in the eight lipid binding sites of cyt b_6f (**Fig. 2B**). The finding that the hydrophobic space occupied by the eighth transmembrane helix of the respiratory and anoxic photosynthetic cytochrome bc_1 complex is occupied by a lipid and a chlorophyll in the b_6f complex raises the question of the pressure in evolution that led to this change [12, 57]. The question is posed of the function of the lipid substitution in relation to the evolutionary change between the eight and seven helix structures of the cyt *b* polypeptide [57]. Based on the known n-side activation of the light harvesting chlorophyll protein kinase by p-side plastoquinol [58], one possibility is that the change was directed by the selective advantage of p- to n-side trans-membrane signaling functions in b_6f, with the lipid either mediating this function, or substituting for the TMH of a signaling protein lost in crystallization.

Assembly of the hetero-oligomeric cyt b_6f complex

As discussed above, the active dimeric cyt b_6f complex consists of at least 8 distinct transmembrane gene products (cyt *f*, cyt b_6, Rieske ISP, subIV, PetG, L, M and N), along with 7 tightly bound prosthetic groups (hemes *f*, b_p, b_n and c_n, [2Fe-2S] cluster, chl-*a* and β-car) (**Figs. 2A, B**). The genes for the subunits do not constitute a single operon. The cyt b_6 gene (*petB*) and the subIV gene (*petD*) are under the genetic control of a single promoter, as the *petBD* operon [59, 60]. In prokaryotes, the ISP gene (*petC*) and the cyt *f* gene (*petA*) are also organized into an operon, the *petCA* operon. Hence, the transcription of the four major subunits is expected to be genetically co-ordinated. However, the four peripheral subunits,

Pet G, L, M and N, are not encoded by genes that are within an operon. Genetic control and coordination of the Pet G, L, M and N synthesis is not well understood.

Mutagenesis studies have provided information about the sequence of events that lead to the assembly of the dimeric cyt b_6f complex [61-69]. Heme binding has been suggested to be an important event in stabilization of the cyt b_6f component polypeptides. In the absence of bound heme moieties, the cyt b_6 and cyt *f* polypeptides are highly sensitive to proteases [63, 64]. An analysis of the cyt b_6f crystal structures shows that the cyt b_6 hemes b_p and b_n are involved in structural stabilization to the cyt b_6 polypeptide. Axial coordination to the hemes b_p and b_n is provided by His86/His187 and His100/His202 respectively of the cyt b_6 polypeptide, which leads to its folding into a compact four helix bundle [2, 3]. Heme-mediated stabilization of the cyt *f* subunit occurs via an unusual ligation of the heme via the Tyr1 residue side-chain of the mature cyt *f* polypeptide [18]. Crystal structures of the isolated cyt *f* extrinsic domain and of the intact dimeric cyt b_6f complex show virtually no structural differences between the cyt *f* extrinsic domain. Hence, heme binding is an important event in the folding and stabilization of the subunits of the cyt b_6f complex.

The hetero-oligomeric nature of the b_6f complex requires the presence of lipids to enhance and strengthen protein-protein interactions between non-identical subunits [52]. Lipids present on the surface and between polypeptide subunits provide cross-linking interactions that contribute to stability of the complex. As discussed elsewhere [12], crystal structures of b_6f show well-defined lipid, detergent and lipidic pigment binding sites. The organization of lipidic molecules within the b_6f complex provides clues to the process of assembly. Given the close interactions between the distinct polypeptides and the integral association of prosthetic groups and lipids with the folded polypeptides, it is important to determine the mode of cyt b_6f assembly in the thylakoid membrane, both in terms of the order in which various subunits are assembled and the stage(s) of insertion of prosthetic groups.

Assembly of a functional cyt b_6f complex dimer would require coordination in time of synthesis of the various subunits in proximity of the synthesized products to ensure that all necessary polypeptides are available to assemble into the functional complex. On the basis of the genetic organization of cyt b_6f and crystal structures of the purified dimeric complex from the cyanobacteria *M. laminosus* (PDB IDs 1VF5, 2E74) [2, 13] and *Nostoc* PCC 7120 (PDB 2ZT9) [5], and *C. reinhardtii* (PDB ID 1Q90) [3], a model is proposed to explain the sequence of events that lead to the formation of the dimeric cyt b_6f complex in thylakoid membranes. The first step is considered to involve the transcriptional activation of the *petBD* operon that encodes the polytopic cyt b_6 and subIV subunits of b_6f that form the core. Following transcription, the mRNA is translated into the cyt b_6 and subIV polypeptides that undergo co-insertion into the membrane to form the polytopic monomeric core of the cyt b_6f complex (**Fig. 5**, **step 1**). Dimerization of the polytopic monomer is expected to follow its assembly. As seen in the crystal structures of the b_6f complex, lipids, and detergents that mark physiological lipid binding sites act as cross-linkers to stabilize monomer-monomer interactions at the interface of the dimer. Three lipid sites mediate inter-monomer interactions, viz., (**i**) p-side lipid, mimicked by the synthetic lipid DOPC (**Fig. 5**, **step 2**, DOPC lipid shown as red sticks) in the *M. laminosus* cyt b_6f structure (PDB ID 1VF5) located at the opening of the inter-monomer cavity, and (**ii, iii**) two n-side UDM detergent

occupied sites (**Fig. 5**, **step 1**, UDM detergent shown as red/white sticks) that interact with the cyt b_6 N-terminus of one monomer and the cyt b_6 D TMH of the other monomer in *M. laminosus* cyt b_6f (PDB ID 2E74) (**Fig. 5**, **step 3**). The ISP and cyt *f* polypeptides are expected to be co-inserted into the thylakoid membrane to form an ISP-cyt *f* sub-complex (**Fig. 5**, **step 4**). The interaction between the two polypeptides is strengthened on the n-side by the native acidic sulfolipid that interacts with basic residues from the trans-membrane helices of ISP and cyt *f*. On the p-side, the ISP-cyt *f* interaction is mediated by another lipid binding site. A detergent and a photosynthetic pigment eicosane were modeled into this site in crystal structures of the b_6f complex from cyanobacteria (PDB IDs 2E74, 2ZT9) and *C. reinhardtii* (PDB ID 1Q90). Van der Waals interactions stabilize the interaction between lipid in the p-side site and the residues of the ISP and cyt *f* TMH. This ISP-cyt *f* sub-complex then interacts with the cyt b_6-subIV polytopic core nucleus to form a cyt b_6-subIV-ISP-cyt *f* sub-complex. As discussed elsewhere, the acidic sulfolipid and the ligand in the p-side lipid site contribute to the association through Van der Waals interactions with residues from the polytopic core. Biochemical evidence supports the existence of an ISP-cyt *f* sub-complex in spinach [70]. The proposed model explains the existence of these smaller complexes as a consequence of proximity between the genes that encode these subunits, which allows for coordination in transcription, translation, membrane insertion and assembly.

The four small subunits of the cyt b_6f complex, Pet G, L, M and N, are organized into a four helix bundle in the structure of the b_6f complex [2, 3, 5, 13]. Pet L, M and N form a β-car binding site. The sequence conservation of these subunits is low. Pet G, the subunit with the highest degree of sequence conservation does not interact with the β-car [12, 71]. Since these subunits are encoded by genes that are separated by large distances, the assembly process would require a long-range communication for coordination between genetic transcription, translation, membrane insertion and assembly. The structure of the b_6f complex shows that on the n-side, the extrinsic portion of these subunits consists of basic amino acid residues [11, 72]. Based on the *cis*-positive rule [73] and the short length of the Pet subunits helices that span the hydrophobic membrane only once, it has been suggested that they are inserted spontaneously into the membrane [72]. It is expected that organization of the Pet subunits around the β-car molecule leads to the formation of the four helix bundle (**Fig. 5**, **step 5**). Assembly of the PetGLMN sub-complex may take place independently on the periphery of the cyt b_6f polytopic core. Mutagenesis studies have shown that Pet G and Pet N, which show relatively high sequence conservation, are essential to the stability of the dimeric b_6f complex [71, 74, 75].

The crystal structure of the cyt b_6f complex shows a clear separation between the polytopic core domain and the peripheral domain that consists of single helix subunits [12]. It is noted that the PetGLMN sub-complex may interact with the ISP-cyt *f* sub-complex (**Fig. 5**, **step 6**), leading to the formation of a peripheral sub-complex that interacts with the polytoptic core, which eventually forms the hetero-oligomeric, fully functional cyt b_6f complex (**Fig. 5**, **step 7**).

Cyt b_6f and super-complex formation

Elucidation of the structural organization of cyt *bc* complexes provided an understanding of the function performed by these quinone oxidoreductases in energy transduction. Sequence conservation of the transmembrane core subunits [6] was found to extend to the structure cyt *bc* complexes, between the cyt *b* polypeptide of the bc_1 complex and the cyt b_6/subIV polypeptides of the cyt b_6f complex (discussed above). A significant and conserved structural feature relates to the organization of the p-side quinol oxidation (Q_p) site. It has been demonstrated that the deprotonation of the semiquinone intermediate within the Q_p-site is mediated by the Glu residue of the conserved PEWY sequence located on the *ef*-loop [76-78]. In the cyt bc_1 complex (PDB ID 3CX5) [79], the *ef*-loop is inserted between the F and G TMH of the cyt *b* subunit (**Fig. 6**, **left panel**). Stabilization of the Q_p-site architecture depends on the 8th C-terminal "H" TMH of the cyt *b* subunit in the bc_1 complex. The helix is inserted in the space between the F and G helices and hence, stabilizes the inter-helix space that is required for the insertion of the *ef*-loop. A very similar structural arrangement of the Q_{p-} site is observed in the b_6f complex (**Fig. 6**, **right panel**). However, it has been noted previously that an unusual evolutionary structural difference between the cyt b_6f and bc_1 complexes is seen in the organization of the cyt *b* polypeptide [12, 57]. The 'H' TMH, which performs an important role of stabilizing the niche for the catalytically important *ef*-loop, is absent from the photosynthetic cyt b_6f complex. As demonstrated, the niche of the missing H TMH is occupied by a lipid and a chl-*a* molecule in the cyt b_6f complex.

Protein-to-lipid substitution: Structure-driven evolutionary modification

Why should a transmembrane helix be replaced by a lipid and a lipid-like chl-*a* molecule? A possible explanation may lie in the pathway of state transitions, which is unique to photosynthesis (**Fig. 7**) [80]. Photosynthetic state transitions balance the redox poise of the plastoquinone (PQ)/plastoquinol (PQH_2) pool within the thylakoid membrane. The Photosystem-II (PSII) reaction center utilizes solar energy to catalyze the reduction of PQ to PQH_2 (**Fig. 7A**). The reduced PQH2 moiety then diffuses to the cyt b_6f complex, where it undergoes oxidation within the Q_p-site. Based on studies performed on the cyt bc_1 complex, quinol oxidation within the Q_p-site of the cyt b_6f complex is expected to constitute the rate limiting step in the photosynthetic electron transport chain. As a result, PQH_2/PQ redox poise shifts to a predominantly reduced state (**Fig. 7B**). To restore balance, an enzyme identified as the LHCII kinase Stt7 in *C. reinhardtii*, is activated [81, 82]. The LHCII kinase phosphorylates the accessory antenna LHC molecules associated with the PSII reaction center, causing their dissociation and migration to photosystem I (PSI). In the absence of LHC molecules, the efficiency of light harvesting and catalysis of PQ reduction by PSII is significantly diminished (**Fig. 7C**). PQH_2 consumption by the cyt b_6f complex is not affected, and hence, redox balance is restored in the PQ/PQH_2 pool. Mutagenesis experiments have shown that the cyt b_6f complex acts as the sensor of the quinone pool redox state [58]. Binding of PQH_2 within the Q_p-site generates a signal that activates the LHCII kinase. Biochemical studies of the Stt7 kinase in *C. reinhardtii* show that the kinase has a membrane spanning domain along with an extrinsic domain on n- side of the thylakoid membrane [81, 82]. Catalytic activity of the LHCII kinase resides in the extrinsic domain, and is activated by PQH_2 binding within cyt b_6f on the p-side of the membrane. The kinase

activating signal has to be transduced across the hydrophobic bilayer. The exact mechanism by which PQH_2 binding generates the signal and the identity of the signal are presently unknown.

LHCII kinase activation: Putative mechanism

A comparative analysis of the cyt b_6f crystal structures from cyanobacteria (PDB IDs 2E74, 2ZT9) and *C. reinhardtii* (PDB ID1Q90) shows an interesting structural feature that may be relevant to transmembrane signal transduction to activate state transitions. The chl-*a* chlorin-ring is inserted between the F and G TMH of subIV (**Fig. 8**). The phytyl-tail of chl-*a* passes through the portal that leads into the Q_p-site for substrate binding. The phytyl-tail of the chl-*a* has different conformations in the crystal structures of cyt b_6f obtained from cyanobacteria (PDB IDs 2E74, 2ZT9) and *C. reinhardtii* (PDB ID 1Q90). In the cyanobacterial cyt b_6f complex, the chl-*a* phytyl tail is wrapped around the F TMH while in the cyt b_6f structure from *C. reinhardtii*, the phytyl-tail is located proximal to the C TMH (**Fig. 8**). The alternate positions indicate potential flexibility in the chl-*a* phytyl-tail. It is proposed that upon binding of the natural substrate plastoquinol-9 within the Q_p-portal of cyt b_6f, the 45 carbon long isoprenoid tail of plastoquinol-9 molecule displaces the chl-*a* phytyl-tail, thereby modifying the interaction between chl-*a* and the 'F' TMH (**Fig. 9**). It is proposed that changes in the chl-*a*/F TMH interaction generate a signal that is transduced to the n-side of the cyt b_6f complex, either directly through the 'F' TMH or by a combinatorial mechanism that involves the 'F' and lipid substituting for the 'H' TMH. The 'F' TMH is the prime candidate for signal transduction as it provides a direct physical connection between the substrate binding Q_p-site on the p-side and the n-side surface of the cyt b_6f complex.

It is significant to note that no structure is available for the isolated, purified LHCII kinase. Biochemical evidence is not available to determine the binding site for the kinase on the cyt b_6f complex. It is possible that the lipid bound between the 'F' and 'G' TMH of cyt b_6f actually represents the LHCII kinase binding site. Crystallographic evidence can be obtained from cyanobacterial crystal structures of the cyt b_6f complex [5, 13] in which DOPC, a non-physiological lipid, is able to bind in the niche. Hence, the lipid binding site between the 'F' and 'G' TMH is not expected to have a very high affinity for lipids. This inference is further supported by the crystal structure of the cyt b_6f complex obtained from *C. reinhardtii* [3]. A long, tubular electron density is observed in the binding niche between the F and G helices, which may belong to lipid present at a low occupancy (**Fig. 10**). Based on these observations of an exchangeable lipid, it is proposed that the niche formed between the F and G TMH may represent the binding site for the LHCII kinase (**Fig. 11**). In this model, the presence of the lipid may represent a state in which the cyt b_6f- LHCII kinase association has not been established. Formation of the cyt b_6f-LHCII kinase super-complex would be accompanied by the replacement of the n-side lipid by the transmembrane domain of the LHCII kinase. The LHCII kinase would interact with the Q_p-site and the F TMH of cyt b_6f. According to the proposed model, replacement of the H TMH of the cyt *b* polypeptide is explained by the need to generate the binding site for the LHCII kinase.

Structure-linked role of β-carotene in cyt b_6f complex

The model of LHCII kinase binding and activation assigns a structural role to the photosynthetic pigment chl-*a*, instead of a photochemical function. This is a unique role that is not commonly observed. In the cyt b_6f complex, in addition to the chl-*a* molecule, one β–car is inserted into the periphery of the complex, in between the peripheral Pet subunits, as described elsewhere [2, 3] and discussed above. Biological systems that harvest light, such as photosystems and light harvesting complex proteins, utilize chlorophyll molecules to capture light and initiate photochemistry. However, in the excited triplet state, the chlorophyll molecule has the potential to transfer energy to molecular oxygen, leading to the formation of harmful reactive oxygen species [83]. β–Car molecules are utilized as quenchers in such biological systems to dissipate energy from the potentially harmful excited triplet state of chlorophyll. However, the separation between the chl-a and the β– car molecule within the cyt b_6f monomer is 14 Å, which is significantly larger than a 4 Å distance that would allow efficient wave-function overlap [84]. It has been suggested that the energy transfer may take place between the chl-*a* and β–car of cyt b_6f via an oxygen-channel [85, 86]. However, experimental demonstration of such a channel remains elusive. As an alternative function, the β–car molecule is thought to perform two structural roles [12, 57]. The β–car molecule may mediate assembly of the heterooligomeric cyt b_6f complex by providing a scaffold for the organization of the PetGLMN sub-complex. Additionally, it has been suggested that the β–car molecule may function as a molecular antenna that mediates the search for other photosynthetic complexes, such as PSI, and then serves as a latch to mediate the formation of a cyt b_6f-PSI super-complex. The isolation of an enzymatically functional cyt b_6f-PSI super-complex has recently been reported from *C. reinhardtii* thylakoid membranes [87]. While the models proposed in the present discussion suggest structural functions for the photosynthetic pigments chl-*a* and β–car, the problem of the large 14 Å separation between the pigment molecules in the cyt b_6f complex still remains. In the absence of a β–car mediated pathway to channel energy from the excited chl-*a* molecule, the cyt b_6f complex is prone to generate reactive harmful species that may cause oxidation of biological molecules. It is expected that a mechanism for energy dissipation from the chl-*a* moiety of cyt b_6f must be operational under *in-vivo* conditions of photosynthetic electron transfer.

Structural studies of the cyt b_6f complex have so far been performed in isolation with crystallization grade purity [50]. While crystallographic studies of the isolated cyt b_6f complex have yielded valuable information, it has not been possible to study the interactions of the cyt b_6f complex with other membrane proteins, such as the photosystems. Within the thylakoid membrane, photosystems, cyt b_6f and LHC complexes do not operate in isolation. Interaction between the large hetero-oligomeric membrane bound complexes mediates physiologically relevant photochemistry and electrochemistry. On these lines, it is possible that the chl-*a* molecule of the cyt b_6f complex is quenched by a β-car from another membrane bound photosynthetic protein, such as a photosystem or an LHC molecule. Such an interaction would require close interaction between cyt b_6f and other membrane bound proteins. With the elucidation of the existence of a cyt b_6f-PSI super-complex [87], evidence has been presented for physical association between the hetero-oligomeric photosynthetic complexes. An analysis of the crystal structures of Photosystems I [88] and II [89, 90] and

of the light harvesting complex II [91] shows that peripheral carotenoids are ubiquitous in these complexes (**Fig. 12**). Hence, it is possible that the formation of a super-complex of the cyt b_6f complex not only mediates metabolic processes, but also provides the necessary pathway for quenching of the chl-*a* excited state within the b_6f complex.

Selectivity (and the lack thereof) in the Q_n-site of cyt b_6f complex

A useful tool in studies of electron transfer through the hemes and [2Fe-2S] cluster prosthetic groups of cyt *bc* complexes has been the use of specific quinone analog inhibitors [92-94]. Inhibitors approximately simulate the binding properties of the natural substrate to occupy the Q_p and Q_n sites of quinol oxidation and quinone reduction on the p and n-sides of cyt *bc* complexes. In the presence of inhibitors, electron transfer is inhibited through the cyt *bc* complexes. Specific inhibitors have been designed to block defined pathways of electron transfer. As a result, characterization of inhibitors has been performed according to their specific role in blocking the process of electron transfer. With regard to the cyt bc_1 complex [94], class I inhibitors include stigmatellin and 5-nundecyl-6-hydroxy-4,7-dioxobenzothioale (UHDBT) that bind within the Q_p-site and interact with the ISP subunit. The binding of class I inhibitors has been characterized to occur in a 'pocket' removed from heme b_p and within H-bond distance of an ISP histidine residue. On the other hand, class II inhibitors include myxothiazole and β-methoxyacrylate stilbene (MOA-stilbene) and famoxadone that bind close to heme b_p and do not interact with the ISP protein significantly, with the exception of famoxadone. Together, the class I and II inhibitors comprise the p-side quinone analog inhibitors that prevent quinol oxidation within the Q_p-portal of the cyt bc_1 complex. On the n-side of the cyt bc_1 complex, one of the most well-characterized and potent inhibitors is antimycin-A. The inhibitor antimycin-A prevents the n-side reaction, i.e., reduction of quinone to quinol bound at the Q_n-site of the cyt bc_1 complex. Distinction of quinone analog inhibitors as p and n-side specific agents is possible from crystallographic studies of cyt bc_1 complex [38, 94, 95]. Crystallographic studies of the purified cyt b_6f complex from the cyanobacterium *M. laminosus* present a different situation [13]. Tridecyl-stigmatellin (TDS), an analog of the cyt bc_1 p-side inhibitor stigmatellin was used for cocrystallization studies. As expected from previous studies, TDS was found to bind at the Q_p-site within the cyt b_6f complex. Surprisingly, electron density for the chromone ring of TDS was also observed on the n-side, bound axially to the unique heme c_n. Binding of TDS at the Q_n-site of cyt b_6f indicates that selectivity of inhibitor binding at the Q_n-site may be less well defined in cyt b_6f compared to the cyt bc_1 complex.

An analysis of the polypeptide environment around the Q_n-site of the cyt b_6f complex provides an explanation for the limited selectivity of inhibitor binding (**Fig. 13**). The Q_n-site in the cyt b_6f complex consists of a heme b_n/c_n couple [13]. The presence of heme c_n extends the binding site of the substrate quinone farther away from the protein environment, into the inter-monomer cavity of the cyt b_6f dimer. Using the TDS molecule bound axially to heme c_n as a marker for the natural quinone, it is found that only six amino acids lie within an interaction distance (i.e., within 4.0 Å) of the TDS chromone ring (**Fig. 13A**). Val26 of cyt b_6 and Ala31, Asp35, Leu36 and Phe40 interact with the TDS chromone ring through Van der Waals interaction. Arg207 of cyt b_6 forms the only selective hydrogen bond interaction with the TDS chromone ring. In contrast, in the cyt bc_1 complex (PDB ID 1KB9)

[36], the ring of the ubiquinone-6 molecule bound at the Q_n-site interacts with seven residues from the cyt *b* polypeptide within a distance of 4.0 Å. Tyr16, Gln22, Trp30, Ser206 and Asp229 form polar interactions with the quinone ring while Leu201 and Met221 interact via Van der Waals interactions (**Fig. 13B**). Hence, selectivity is larger in the cyt bc_1 complex due to the larger fraction of selective polar interactions. This structural feature may also explain the observation that no quinone analog inhibitor for the cyt b_6f Q_n-site has been found to be comparable in efficiency to antimycin bound at the Q_n-site of cyt bc_1 [92]. It is inferred that binding of ligands and quinone analog inhibitors at the Q_n-site is less selective in the b_6f complex than in the bc_1 complex, mainly due to fewer interactions.

Abbreviations

β-Car	β-carotene
Chl-*a*$^-$	chlorophyll-*a*
Cyt	cytochrome
Em7	midpoint oxidation-reduction potential at pH 7
$\Delta\tilde{\mu}H+$	trans-membrane proton electrochemical potential gradient
n, p-sides	electrochemically negative and positive side of the membrane
PDB	protein data bank
PC	plastocyanin
PQ	plastoquinone
PS	photosystem
subIV	subunit IV of the b_6f complex
TMH	transmembrane helix

Bibliography and Literature Cited

1. Nelson N, Ben-Shem A. The complex architecture of oxygenic photosynthesis, Nature reviews. Molecular cell biology. 2004; 5:971–982. [PubMed: 15573135]
2. Kurisu G, Zhang H, Smith JL, Cramer WA. Structure of the cytochrome b6f complex of oxygenic photosynthesis: tuning the cavity. Science. 2003; 302:1009–1014. [PubMed: 14526088]
3. Stroebel D, Choquet Y, Popot JL, Picot D. An atypical haem in the cytochrome b(6)f complex. Nature. 2003; 426:413–418. [PubMed: 14647374]
4. Allen JF. Cytochrome b6f: structure for signalling and vectorial metabolism. Trends in plant science. 2004; 9:130–137. [PubMed: 15003236]
5. Baniulis D, Yamashita E, Whitelegge JP, Zatsman AI, Hendrich MP, Hasan SS, Ryan CM, Cramer WA. Structure-Function, Stability, and Chemical Modification of the Cyanobacterial Cytochrome b6f Complex from Nostoc sp. PCC 7120. The Journal of biological chemistry. 2009; 284:9861–9869. [PubMed: 19189962]
6. Widger WR, Cramer WA, Herrmann RG, Trebst A. Sequence homology and structural similarity between cytochrome b of mitochondrial complex III and the chloroplast b6-f complex: position of the cytochrome b hemes in the membrane. Proceedings of the National Academy of Sciences of the United States of America. 1984; 81:674–678. [PubMed: 6322162]

7. Zatsman AI, Zhang H, Gunderson WA, Cramer WA, Hendrich MP. Heme-heme interactions in the cytochrome b6f complex: EPR spectroscopy and correlation with structure. Journal of the American Chemical Society. 2006; 128:14246–14247. [PubMed: 17076484]
8. Twigg AI, Baniulis D, Cramer WA, Hendrich MP. EPR detection of an O(2) surrogate bound to heme c(n) of the cytochrome b(6)f complex. Journal of the American Chemical Society. 2009; 131:12536–12537. [PubMed: 19689132]
9. Alric J, Pierre Y, Picot D, Lavergne J, Rappaport F. Spectral and redox characterization of the heme ci of the cytochrome b6f complex. Proceedings of the National Academy of Sciences of the United States of America. 2005; 102:15860–15865. [PubMed: 16247018]
10. Cramer WA, Zhang H. Consequences of the structure of the cytochrome b6f complex for its charge transfer pathways. Biochimica et biophysica acta. 2006; 1757:339–345. [PubMed: 16787635]
11. Cramer WA, Zhang H, Yan J, Kurisu G, Smith JL. Transmembrane traffic in the cytochrome b6f complex. Annual review of biochemistry. 2006; 75:769–790.
12. Hasan SS, Yamashita E, Ryan CM, Whitelegge JP, Cramer WA. Conservation of lipid functions in cytochrome bc complexes. Journal of molecular biology. 2011; 414:145–162. [PubMed: 21978667]
13. Yamashita E, Zhang H, Cramer WA. Structure of the cytochrome b6f complex: quinone analogue inhibitors as ligands of heme cn. Journal of molecular biology. 2007; 370:39–52. [PubMed: 17498743]
14. Sainz G, Carrell CJ, Ponamarev MV, Soriano GM, Cramer WA, Smith JL. Interruption of the internal water chain of cytochrome f impairs photosynthetic function. Biochemistry. 2000; 39:9164–9173. [PubMed: 10924110]
15. Chi YI, Huang LS, Zhang ZL, Fernandez-Velasco JG, Berry EA. X-ray structure of a truncated form of cytochrome f from Chlamydomonas reinhardtii. Biochemistry. 2000; 39:7689–7701. [PubMed: 10869174]
16. Carrell CJ, Schlarb BG, Bendall DS, Howe CJ, Cramer WA, Smith JL. Structure of the soluble domain of cytochrome f from the cyanobacterium Phormidium laminosum. Biochemistry. 1999; 38:9590–9599. [PubMed: 10423236]
17. Ubbink M, Ejdeback M, Karlsson BG, Bendall DS. The structure of the complex of plastocyanin and cytochrome f, determined by paramagnetic NMR and restrained rigid-body molecular dynamics. Structure. 1998; 6:323–335. [PubMed: 9551554]
18. Martinez SE, Huang D, Szczepaniak A, Cramer WA, Smith JL. Crystal structure of chloroplast cytochrome f reveals a novel cytochrome fold and unexpected heme ligation. Structure. 1994; 2:95–105. [PubMed: 8081747]
19. Martinez SE, Huang D, Ponomarev M, Cramer WA, Smith JL. The heme redox center of chloroplast cytochrome f is linked to a buried five-water chain. Protein Sci. 1996; 5:1081–1092. [PubMed: 8762139]
20. Veit S, Takeda K, Tsunoyama Y, Rexroth D, Rogner M, Miki K. Structure of a thermophilic cyanobacterial b6f-type Rieske protein. Acta Crystallogr D. 2012; 68:1400–1408. [PubMed: 22993094]
21. Carrell CJ, Zhang H, Cramer WA, Smith JL. Biological identity and diversity in photosynthesis and respiration: structure of the lumen-side domain of the chloroplast Rieske protein. Structure. 1997; 5:1613–1625. [PubMed: 9438861]
22. Cramer WA, Martinez SE, Huang D, Tae GS, Everly RM, Heymann JB, Cheng RH, Baker TS, Smith JL. Structural aspects of the cytochrome b6f complex; structure of the lumen-side domain of cytochrome f. Journal of bioenergetics and biomembranes. 1994; 26:31–47. [PubMed: 8027021]
23. Schutz M, Brugna M, Lebrun E, Baymann F, Huber R, Stetter KO, Hauska G, Toci R, Lemesle-Meunier D, Tron P, Schmidt C, Nitschke W. Early evolution of cytochrome bc complexes. Journal of molecular biology. 2000; 300:663–675. [PubMed: 10891261]
24. Yan J, Cramer WA. Functional insensitivity of the cytochrome b6f complex to structure changes in the hinge region of the Rieske iron-sulfur protein. The Journal of biological chemistry. 2003; 278:20925–20933. [PubMed: 12672829]
25. Hasan SS, Cramer WA. On rate limitations of electron transfer in the photosynthetic cytochrome b(6)f complex. Phys Chem Chem Phys. 2012; 14:13853–13860. [PubMed: 22890107]

26. Darrouzet E, Cooley JW, Daldal F. The Cytochrome bc (1) Complex and its Homologue the b (6) f Complex: Similarities and Differences. Photosynth Res. 2004; 79:25–44. [PubMed: 16228398]
27. Berry EA, Guergova-Kuras M, Huang LS, Crofts AR. Structure and function of cytochrome bc complexes. Annual review of biochemistry. 2000; 69:1005–1075.
28. Cape JL, Bowman MK, Kramer DM. Understanding the cytochrome bc complexes by what they don't do. The Q-cycle at 30. Trends in plant science. 2006; 11:46–55. [PubMed: 16352458]
29. Mitchell P. Chemiosmotic coupling in oxidative and photosynthetic phosphorylation. Biological reviews of the Cambridge Philosophical Society. 1966; 41:445–502. [PubMed: 5329743]
30. Mitchell P. Protonmotive redox mechanism of the cytochrome b-c1 complex in the respiratory chain: protonmotive ubiquinone cycle. FEBS letters. 1975; 56:1–6. [PubMed: 239860]
31. Malkin R. Cytochrome-Bc(1) and Cytochrome-B(6)F Complexes of Photosynthetic Membranes. Photosynth Res. 1992; 33:121–136. [PubMed: 24408573]
32. Hurt EC, Gabellini N, Shahak Y, Lockau W, Hauska G. Extra Proton Translocation and Membrane-Potential Generation Universal Properties of Cytochrome Bc1/B6f Complexes Reconstituted into Liposomes. Archives of biochemistry and biophysics. 1983; 225:879–885. [PubMed: 6312896]
33. Zhang H, Whitelegge JP, Cramer WA. Ferredoxin:NADP+ oxidoreductase is a subunit of the chloroplast cytochrome b6f complex. The Journal of biological chemistry. 2001; 276:38159–38165. [PubMed: 11483610]
34. Crofts AR, Guergova-Kuras M, Kuras R, Ugulava N, Li J, Hong S. Proton-coupled electron transfer at the Q(o) site: what type of mechanism can account for the high activation barrier? Biochimica et biophysica acta. 2000; 1459:456–466. [PubMed: 11004463]
35. Crofts AR, Wang ZG. How Rapid Are the Internal Reactions of the Ubiquinol-Cytochrome-C2 Oxidoreductase. Photosynth Res. 1989; 22:69–87. [PubMed: 24424680]
36. Lange C, Nett JH, Trumpower BL, Hunte C. Specific roles of protein-phospholipid interactions in the yeast cytochrome bc1 complex structure. The EMBO journal. 2001; 20:6591–6600. [PubMed: 11726495]
37. Xia D, Deng KP, Kim H, Kachurin A, Yu CA, Yu L, Deisenhofer J. Crystallographic analysis of core proteins of cytochrome b/c1 complex - Implication to the structure and function of mitochondrial processing peptidase. Biophys J. 1997; 72:Th363–Th363.
38. Gao X, Wen X, Esser L, Quinn B, Yu L, Yu CA, Xia D. Structural basis for the quinone reduction in the bc1 complex: a comparative analysis of crystal structures of mitochondrial cytochrome bc1 with bound substrate and inhibitors at the Qi site. Biochemistry. 2003; 42:9067–9080. [PubMed: 12885240]
39. Cramer WA, Hasan SS, Yamashita E. The Q cycle of cytochrome bc complexes: a structure perspective. Biochimica et biophysica acta. 2011; 1807:788–802. [PubMed: 21352799]
40. Seddon AM, Curnow P, Booth PJ. Membrane proteins, lipids and detergents: not just a soap opera. Biochimica et biophysica acta. 2004; 1666:105–117. [PubMed: 15519311]
41. Adamian L, Naveed H, Liang J. Lipid-binding surfaces of membrane proteins: evidence from evolutionary and structural analysis. Biochimica et biophysica acta. 2011; 1808:1092–1102. [PubMed: 21167813]
42. Liang J, Naveed H, Jimenez-Morales D, Adamian L, Lin M. Computational studies of membrane proteins: Models and predictions for biological understanding. Biochimica et biophysica acta. 2012; 1818:927–941. [PubMed: 22051023]
43. Vergis JM, Purdy MD, Wiener MC. A high-throughput differential filtration assay to screen and select detergents for membrane proteins. Analytical biochemistry. 2010; 407:1–11. [PubMed: 20667442]
44. Nussberger S, Dorr K, Wang DN, Kuhlbrandt W. Lipid-Protein Interactions in Crystals of Plant Light-Harvesting Complex. Journal of molecular biology. 1993; 234:347–356. [PubMed: 8230219]
45. Cartailler JP, Luecke H. X-ray crystallographic analysis of lipid-protein interactions in the bacteriorhodopsin purple membrane. Annual review of biophysics and biomolecular structure. 2003; 32:285–310.

46. Escriba PV, Wedegaertner PB, Goni FM, Vogler O. Lipid-protein interactions in GPCR-associated signaling. Bba-Biomembranes. 2007; 1768:836–852. [PubMed: 17067547]
47. Hite RK, Li ZL, Walz T. Principles of membrane protein interactions with annular lipids deduced from aquaporin-0 2D crystals. Embo Journal. 2010; 29:1652–1658. [PubMed: 20389283]
48. Qin L, Hiser C, Mulichak A, Garavito RM, Ferguson-Miller S. Identification of conserved lipid/detergent-binding sites in a high-resolution structure of the membrane protein cytochrome c oxidase. Proceedings of the National Academy of Sciences of the United States of America. 2006; 103:16117–16122. [PubMed: 17050688]
49. Qin L, Sharpe MA, Garavito RM, Ferguson-Miller S. Conserved lipid-binding sites in membrane proteins: a focus on cytochrome c oxidase. Current opinion in structural biology. 2007; 17:444–450. [PubMed: 17719219]
50. Zhang H, Kurisu G, Smith JL, Cramer WA. A defined protein-detergent-lipid complex for crystallization of integral membrane proteins: The cytochrome b6f complex of oxygenic photosynthesis. Proceedings of the National Academy of Sciences of the United States of America. 2003; 100:5160–5163. [PubMed: 12702760]
51. Baniulis D, Yamashita E, Zhang H, Hasan SS, Cramer WA. Structure-function of the cytochrome b6f complex. Photochemistry and photobiology. 2008; 84:1349–1358. [PubMed: 19067956]
52. Zhang H, Cramer WA. Problems in obtaining diffraction-quality crystals of hetero oligomeric integral membrane proteins. Journal of structural and functional genomics. 2005; 6:219–223. [PubMed: 16211522]
53. Zhang H, Cramer WA. Purification and crystallization of the cytochrome b6f complex in oxygenic photosynthesis. Methods in molecular biology. 2004; 274:67–78. [PubMed: 15187270]
54. Baniulis D, Zhang H, Zakharova T, Hasan SS, Cramer WA. Purification and crystallization of the cyanobacterial cytochrome b6f complex. Methods in molecular biology. 2011; 684:65–77. [PubMed: 20960122]
55. Breyton C, Tribet C, Olive J, Dubacq JP, Popot JL. Dimer to monomer conversion of the cytochrome b(6)f complex - Causes and consequences. Journal of Biological Chemistry. 1997; 272:21892–21900. [PubMed: 9268322]
56. Pierre Y, Breyton C, Kramer D, Popot JL. Purification and Characterization of the Cytochrome B(6)F Complex from Chlamydomonas-Reinhardtii. Journal of Biological Chemistry. 1995; 270:29342–29349. [PubMed: 7493968]
57. Hasan SS, Cramer WA. Lipid functions in cytochrome bc complexes: an odd evolutionary transition in a membrane protein structure, Philosophical transactions of the Royal Society of London. Series B. Biological sciences. 2012; 367:3406–3411. [PubMed: 23148267]
58. Zito F, Finazzi G, Delosme R, Nitschke W, Picot D, Wollman FA. The Qo site of cytochrome b6f complexes controls the activation of the LHCII kinase. The EMBO journal. 1999; 18:2961–2969. [PubMed: 10357809]
59. Kallas T, Malkin R. Isolation and characterization of genes for cytochrome b6/f complex. Methods Enzymol. 1988; 167:779–794. [PubMed: 2976872]
60. Kallas T, Spiller S, Malkin R. Characterization of two operons encoding the cytochrome b6-f complex of the cyanobacterium Nostoc PCC 7906. Highly conserved sequences but different gene organization than in chloroplasts. The Journal of biological chemistry. 1988; 263:14334–14342. [PubMed: 2844767]
61. Majeran W, Wollman FA, Vallon O. Evidence for a role of ClpP in the degradation of the chloroplast cytochrome b(6)f complex. The Plant cell. 2000; 12:137–150. [PubMed: 10634913]
62. Choquet Y, Stern DB, Wostrikoff K, Kuras R, Girard-Bascou J, Wollman FA. Translation of cytochrome f is autoregulated through the 5′ untranslated region of petA mRNA in Chlamydomonas chloroplasts. Proceedings of the National Academy of Sciences of the United States of America. 1998; 95:4380–4385. [PubMed: 9539745]
63. Kuras R, Buschlen S, Wollman FA. Maturation of Pre-Apocytochrome-F in-Vivo - a Site-Directed Mutagenesis Study in Chlamydomonas-Reinhardtii. Journal of Biological Chemistry. 1995; 270:27797–27803. [PubMed: 7499249]

64. Kuras R, de Vitry C, Choquet Y, Girard-Bascou J, Culler D, Buschlen S, Merchant S, Wollman FA. Molecular genetic identification of a pathway for heme binding to cytochrome b(6). Journal of Biological Chemistry. 1997; 272:32427–32435. [PubMed: 9405452]
65. Kuras R, Wollman FA. The Assembly of Cytochrome B(6)/F Complexes - an Approach Using Genetic-Transformation of the Green-Alga Chlamydomonas-Reinhardtii. Embo Journal. 1994; 13:1019–1027. [PubMed: 8131736]
66. Lemaire C, Girardbascou J, Wollman FA, Bennoun P. Studies on the Cytochrome B6/F Complex . 1. Characterization of the Complex Subunits in Chlamydomonas-Reinhardtii. Biochimica et biophysica acta. 1986; 851:229–238.
67. Kuras R, Wollman FA, Joliot P. Conversion of Cytochrome-F to a Soluble Form in-Vivo in Chlamydomonas-Reinhardtii. Biochemistry. 1995; 34:7468–7475. [PubMed: 7779790]
68. Wollman FA, Kuras R, Choquet Y. Epistatic effects in thylakoid protein synthesis: The example of cytochrome f. Photosynthesis: From Light to Biosphere. 1995; Iii:737–742.
69. Zito F, Kuras R, Choquet Y, Kossel H, Wollman FA. Mutations of cytochrome b(6) in Chlamydomonas reinhardtii disclose the functional significance for a proline to leucine conversion by petB editing in maize and tobacco. Plant molecular biology. 1997; 33:79–86. [PubMed: 9037161]
70. el-Demerdash M, Salnikow J, Vater J. Evidence for a cytochrome f-Rieske protein subcomplex in the cytochrome b6f system from spinach chloroplasts. Archives of biochemistry and biophysics. 1988; 260:408–415. [PubMed: 3277532]
71. Schwenkert S, Legen J, Takami T, Shikanai T, Herrmann RG, Meurer J. Role of the low-molecular-weight subunits PetL, PetG, and PetN in assembly, stability, and dimerization of the cytochrome b6f complex in tobacco. Plant physiology. 2007; 144:1924–1935. [PubMed: 17556510]
72. Cramer WA, Yan J, Zhang H, Kurisu G, Smith JL. Structure of the cytochrome b6f complex: new prosthetic groups, Q-space, and the ‘hors d'oeuvres hypothesis’ for assembly of the complex. Photosynth Res. 2005; 85:133–143. [PubMed: 15977064]
73. Krishtalik LI, Cramer WA. On the Physical Basis for the Cis-Positive Rule Describing Protein Orientation in Biological-Membranes. FEBS letters. 1995; 369:140–143. [PubMed: 7649246]
74. Schneider D, Berry S, Rich P, Seidler A, Rogner M. A regulatory role of the PetM subunit in a cyanobacterial cytochrome b6f complex. The Journal of biological chemistry. 2001; 276:16780–16785. [PubMed: 11278512]
75. Schneider D, Volkmer T, Rogner M. PetG and PetN, but not PetL, are essential subunits of the cytochrome b6f complex from Synechocystis PCC 6803. Research in microbiology. 2007; 158:45–50. [PubMed: 17224258]
76. Zito F, Finazzi G, Joliot P, Wollman FA. Glu78, from the conserved PEWY sequence of subunit IV, has a key function in cytochrome b6f turnover. Biochemistry. 1998; 37:10395–10403. [PubMed: 9671508]
77. Izrailev S, Crofts AR, Berry EA, Schulten K. Steered molecular dynamics simulation of the Rieske subunit motion in the cytochrome bc(1) complex. Biophys J. 1999; 77:1753–1768. [PubMed: 10512801]
78. Victoria D, Burton R, Crofts AR. Role of the -PEWY-glutamate in catalysis at the Q(o)-site of the Cyt bc(1) complex. Biochimica et biophysica acta. 2012
79. Solmaz SR, Hunte C. Structure of complex III with bound cytochrome c in reduced state and definition of a minimal core interface for electron transfer. The Journal of biological chemistry. 2008; 283:17542–17549. [PubMed: 18390544]
80. Rochaix JD. Regulation of photosynthetic electron transport. Biochimica et biophysica acta. 2011; 1807:375–383. [PubMed: 21118674]
81. Lemeille S, Willig A, Depege-Fargeix N, Delessert C, Bassi R, Rochaix JD. Analysis of the Chloroplast Protein Kinase Stt7 during State Transitions. PLoS biology. 2009; 7:664–675.
82. Depege N, Bellafiore S, Rochaix JD. Role of chloroplast protein kinase Stt7 in LHCII phosphorylation and state transition in Chlamydomonas. Science. 2003; 299:1572–1575. [PubMed: 12624266]

83. Cramer WA, Savikhin S, Yan JS, Yamashita E. The Enigmatic Chlorophyll a Molecule in the Cytochrome b(6)f Complex. Chloroplast: Basics and Applications. 2010; 31:89–93.
84. Dexter DL. A Theory of Sensitized Luminescence in Solids. J Chem Phys. 1953; 21:836–850.
85. Dashdorj N, Zhang H, Kim H, Yan J, Cramer WA, Savikhin S. The single chlorophyll a molecule in the cytochrome b6f complex: unusual optical properties protect the complex against singlet oxygen. Biophys J. 2005; 88:4178–4187. [PubMed: 15778449]
86. Yan J, Dashdorj N, Baniulis D, Yamashita E, Savikhin S, Cramer WA. On the structural role of the aromatic residue environment of the chlorophyll a in the cytochrome b6f complex. Biochemistry. 2008; 47:3654–3661. [PubMed: 18302324]
87. Iwai M, Takizawa K, Tokutsu R, Okamuro A, Takahashi Y, Minagawa J. Isolation of the elusive supercomplex that drives cyclic electron flow in photosynthesis. Nature. 2010; 464:1210–1213. [PubMed: 20364124]
88. Jordan P, Fromme P, Witt HT, Klukas O, Saenger W, Krauss N. Three-dimensional structure of cyanobacterial photosystem I at 2.5 angstrom resolution. Nature. 2001; 411:909–917. [PubMed: 11418848]
89. Umena Y, Kawakami K, Shen JR, Kamiya N. Crystal structure of oxygen-evolving photosystem II at a resolution of 1.9 A. Nature. 2011; 473:55–60. [PubMed: 21499260]
90. Guskov A, Kern J, Gabdulkhakov A, Broser M, Zouni A, Saenger W. Cyanobacterial photosystem II at 2.9-angstrom resolution and the role of quinones, lipids, channels and chloride. Nature structural & molecular biology. 2009; 16:334–342.
91. Standfuss J, Terwisscha van Scheltinga AC, Lamborghini M, Kuhlbrandt W. Mechanisms of photoprotection and nonphotochemical quenching in pea light-harvesting complex at 2.5 A resolution. The EMBO journal. 2005; 24:919–928. [PubMed: 15719016]
92. von Jagow G, Link TA. Use of specific inhibitors on the mitochondrial bc1 complex. Methods Enzymol. 1986; 126:253–271. [PubMed: 2856132]
93. Crofts AR, Guergova-Kuras M, Huang L, Kuras R, Zhang Z, Berry EA. Mechanism of ubiquinol oxidation by the bc(1) complex: role of the iron sulfur protein and its mobility. Biochemistry. 1999; 38:15791–15806. [PubMed: 10625445]
94. Crofts AR, Barquera B, Gennis RB, Kuras R, Guergova-Kuras M, Berry EA. Mechanism of ubiquinol oxidation by the bc(1) complex: different domains of the quinol binding pocket and their role in the mechanism and binding of inhibitors. Biochemistry. 1999; 38:15807–15826. [PubMed: 10625446]
95. Gao X, Wen X, Yu C, Esser L, Tsao S, Quinn B, Zhang L, Yu L, Xia D. The crystal structure of mitochondrial cytochrome bc1 in complex with famoxadone: the role of aromatic-aromatic interaction in inhibition. Biochemistry. 2002; 41:11692–11702. [PubMed: 12269811]
96. Kleywegt GJ, Harris MR, Zou JY, Taylor TC, Wahlby A, Jones TA. The Uppsala Electron-Density Server, Acta crystallographica. Section D. Biological crystallography. 2004; 60:2240–2249. [PubMed: 15572777]

Highlights

- We compare cytochrome b_6f and bc_1 crystal structures to identify novel lipid functions.
- The role of lipids in mediating assembly of the b_6f complex is discussed.
- A lipid mediated transmembrane signaling mechanism is suggested for photosynthetic state transitions.

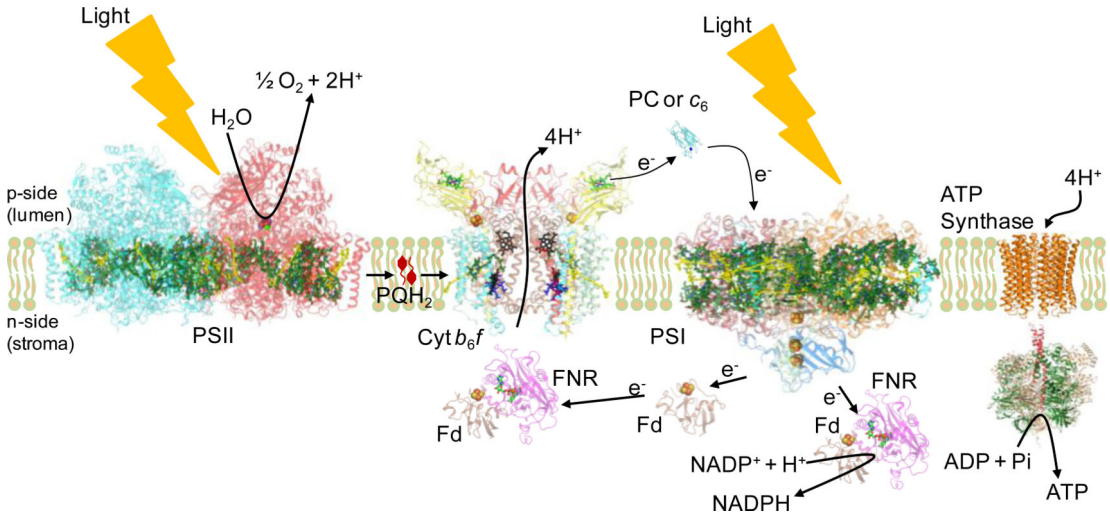

Figure 1. The electron transport chain of oxygenic photosynthesis

Formation of the transmembrane proton electrochemical gradient coupled to the electron transport extending from H_2O oxidation to $NADP^+$ reduction, in which H^+ is translocated in the protein complexes of the PSII reaction center and cytochrome b_6f; this H^+ gradient is utilized for ATP synthesis by the ATP synthase. PDB accession for structure data: Cyt b_6f (PDB ID 2E74), Fd (PDB ID 1EWY), ferredoxin; FNR (PDB ID 1EWY), ferredoxin-$NADP^+$-reductase; PC (PDB ID 2Q5B), plastocyanin; PSII (PDB ID 3ARC) and PSI (PDB ID 1JB0), reaction center complexes.

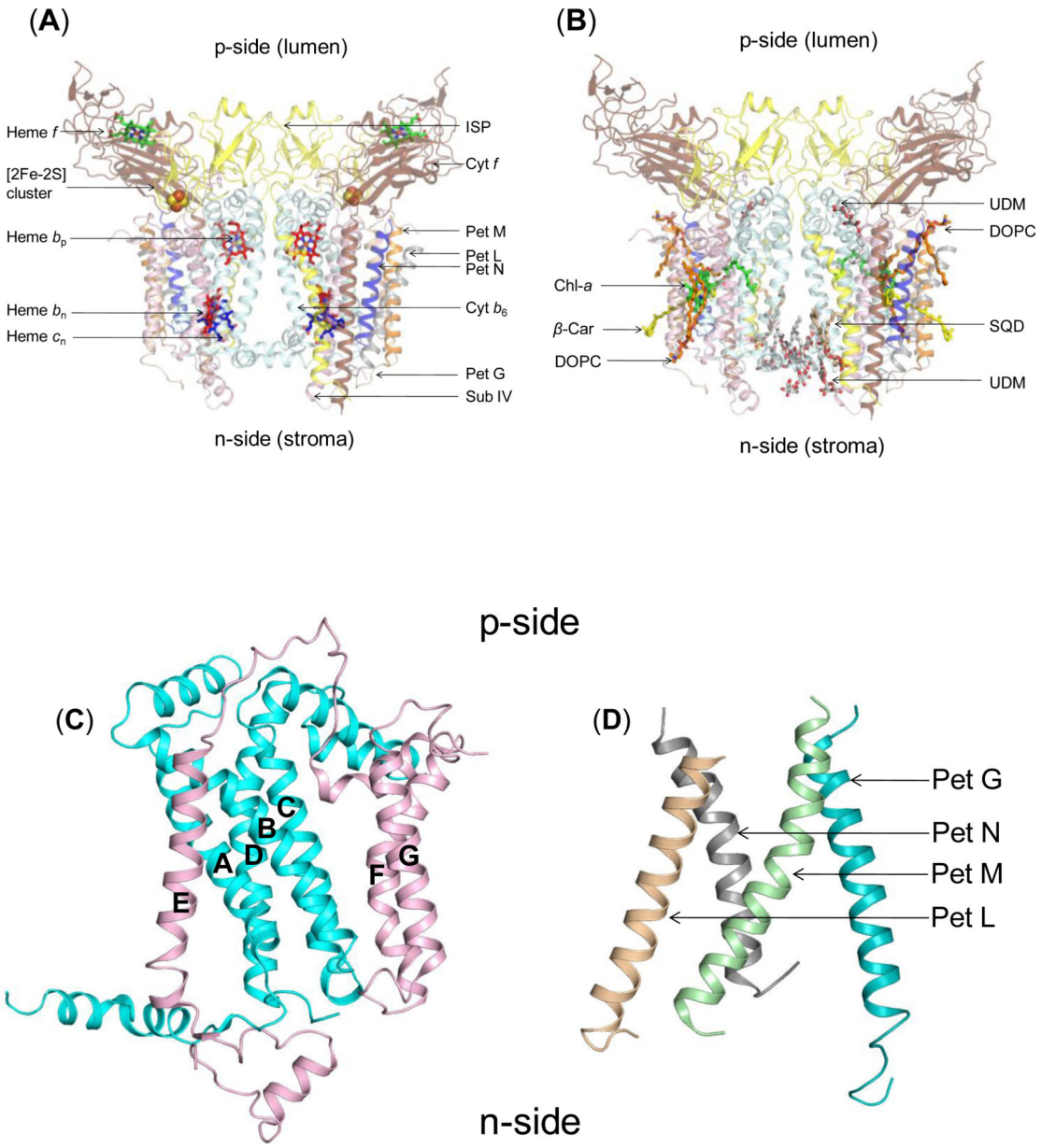

Figure 2. Structure of dimeric b_6f complex from M.laminosus (PDB ID 2E74)

(240,000 MW; per monomer, 8 subunits/7 prosthetic groups; 8 lipids) Subunit organization and lipid binding sites. (**A**) View along membrane plane showing the positions of the 8 subunits. Color code: cytochrome *f* (pet A), yellow; cytochrome b_6 (pet B), cyan); Rieske [2Fe-2S] protein (Pet C), orange; subunit IV/Pet D (pink), Pet G (teal), Pet L (light brown), Pet M (green) and Pet N (gray). (**B**) Side view of *M. laminosus* b_6f complex showing bound lipids, detergents and pigments. (**C**) Polytopic core of the b_6f complex. Cyt b_6 (4 TMH, cyan) and subunit IV (3 TMH, pink) form the core of the b_6f monomer. The cytb_6TMH form a four helix bundle. SubIV is organized around the bundle as a bipartite structure, with the E-helix separated from the F and G TMH. (**D**) Peripheral four helix bundle formed by the small Pet subunits, Pet G, L, M and N. In addition, including ferredoxin-$NADP^+$-reductase (FNR), which may mediate electron transfer from PSI to cyt b_6f. (**Fig. 1**) In addition, there

are four soluble subunits that associate with purified b_6f complex from plant or algal sources, but have not been seen in the crystal structures and have presumably dissociated and been lost during crystallization: the Pet P polypeptide seen in cyanobacteria, the light-harvesting LHCII chlorophyll protein kinase Stt7-STN7, the correlated phosphatase, and the PetO nuclear-encoded phosphorylatable subunit,.

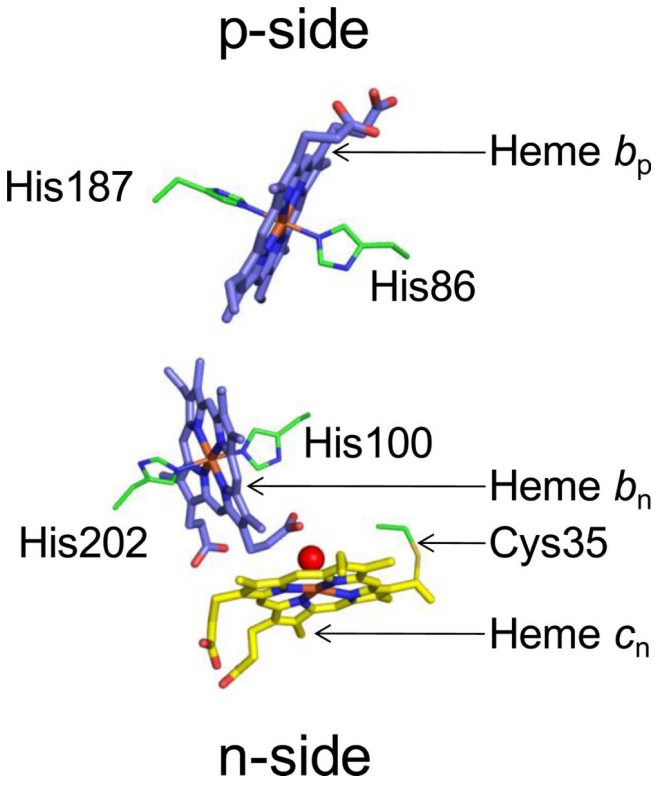

Figure 3. Transmembrane heme organization within cyt b_6f

Three hemes, b_p, b_n and c_n, are located within the b_6f hydrophobic core. Hemes b_p and b_n are axially ligated by histidines from cyt b_6. Heme c_n, a unique heme without an amino acid axial ligand, is linked to a conserved Cys35 residue of cyt b_6, and is axially ligated by a water or hydroxide molecule (red sphere).

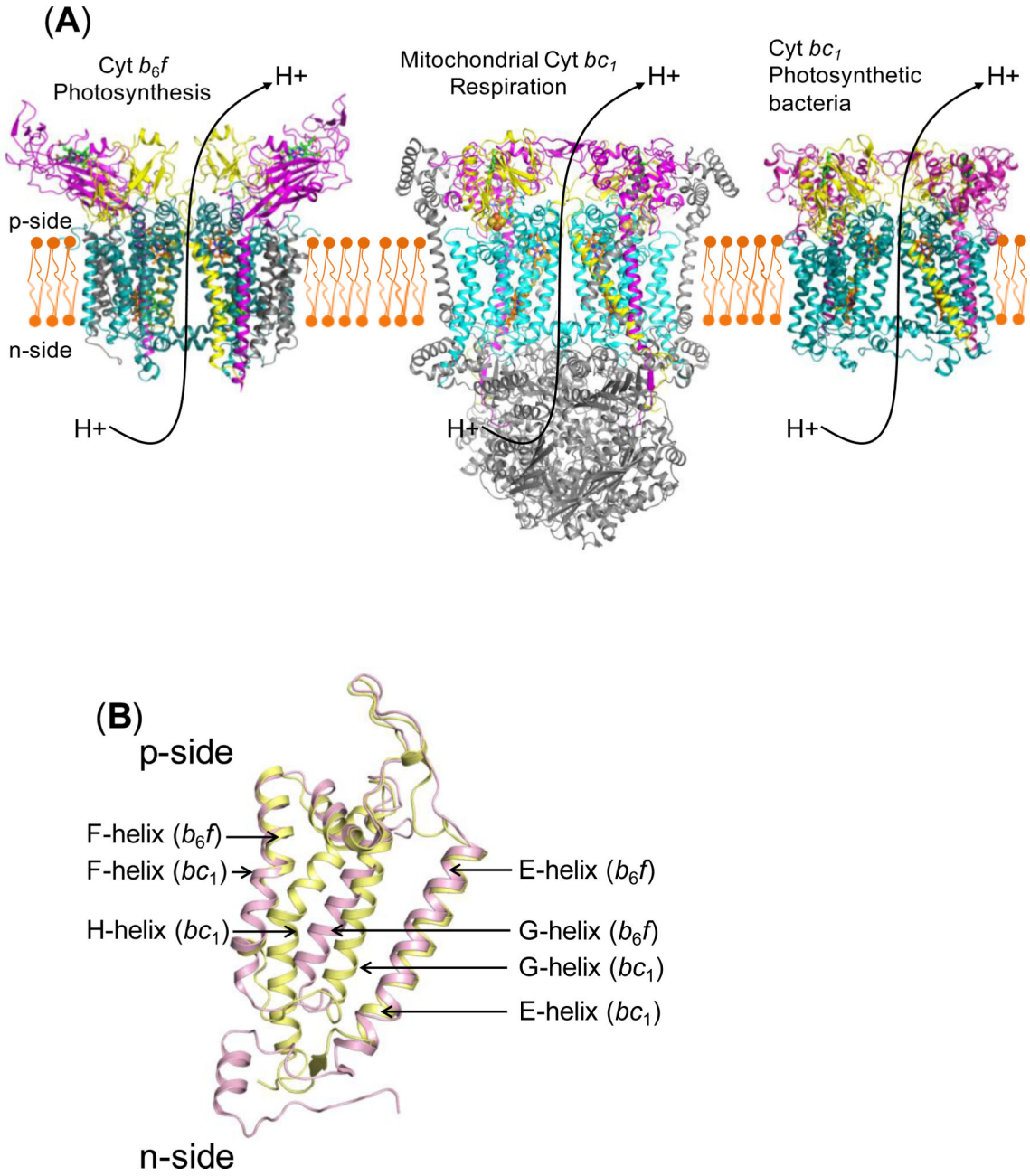

Figure 4. Family of cyt bc complexes

(**A**) Cyt b_6f and the bc_1 complex of mitochondria and anoxygenic photosynthetic bacteria constitute the cyt *bc* family. The transmembrane core (teal) of the *bc* complexes is highly conserved. The complexes catalyze quinone reduction-protonation and quinol deprotonation-oxidation, respectively, on the electrochemically negative and positive sides of the membrane to generate the proton electrochemical potential gradient. (**B**) Structural differences in the core: C-terminal domain of the bc_1 cyt *b* subunit (4 TMH, yellow) has a TMH organization that differs from subIV (3 TMH, pink) of the b_6f complex, although amino acid sequences are highly conserved.

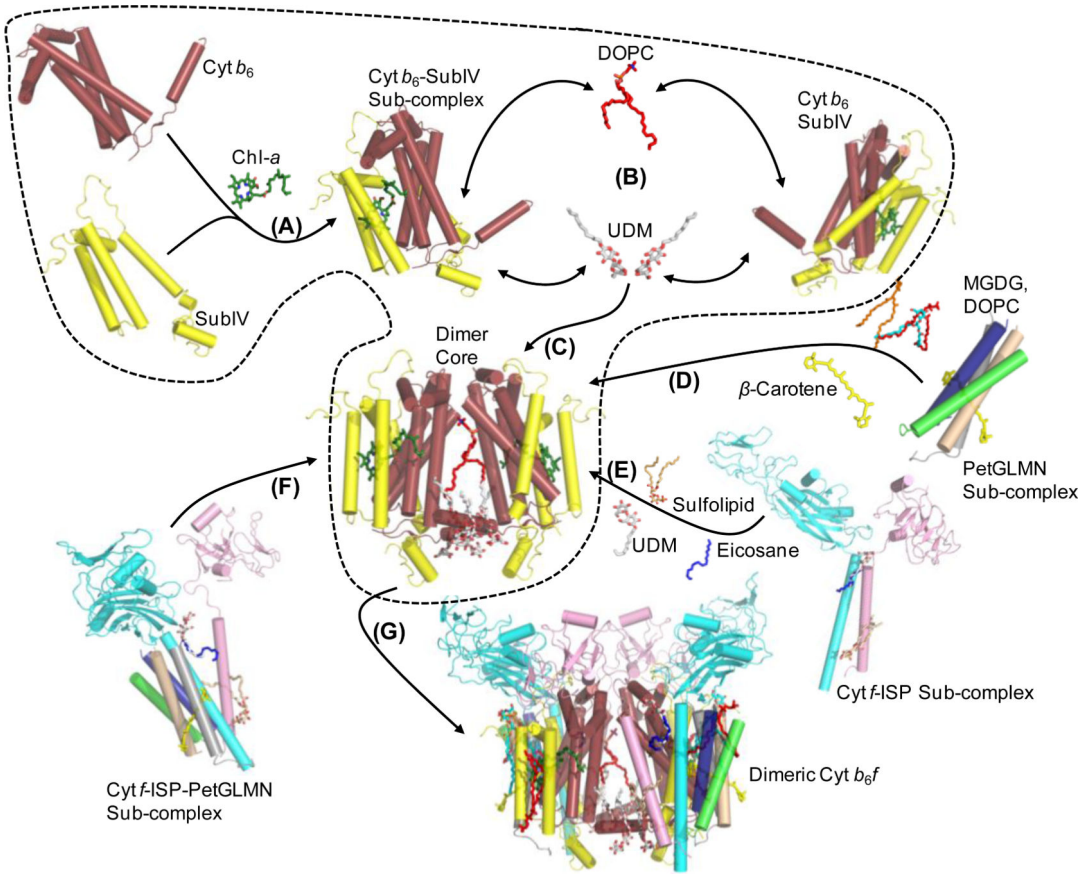

Figure 5. Proposed model for assembly of the cyt b_6f complex

(**Step 1**) The first step involves the assembly of the monomeric polytopic core of cyt b_6 and subIV. (**Step 2**) The monomeric polytopic core then undergoes dimerization, mediated by the cross-linking interactions of lipids (DOPC, shown as red sticks; UDM shown as red/white sticks), which leads to the formation of the dimeric cyt b_6-subIV polytopic core (**Step 3**). Formation of the ISP-cyt *f* sub-complex takes place via the stabilizing interactions of lipids (**Step 4**). Assembly of the PetGLMN sub-complex takes place around the β-carotene molecule (**Step 5**). Interaction of the PetGLMN sub-complex with the core polytopic core takes place via the β-carotene and lipids (sulfolipid, DOPC, MGDG). Alternatively, formation of an ISP-cyt *f*-PetGLMN sub-complex may take place prior to interaction with the dimeric core (**Step 6**). (**Step 7**) Interaction of the peripheral sub-complex with the dimeric core would lead to the formation of the fully assembled, functional dimeric cyt b_6f complex.

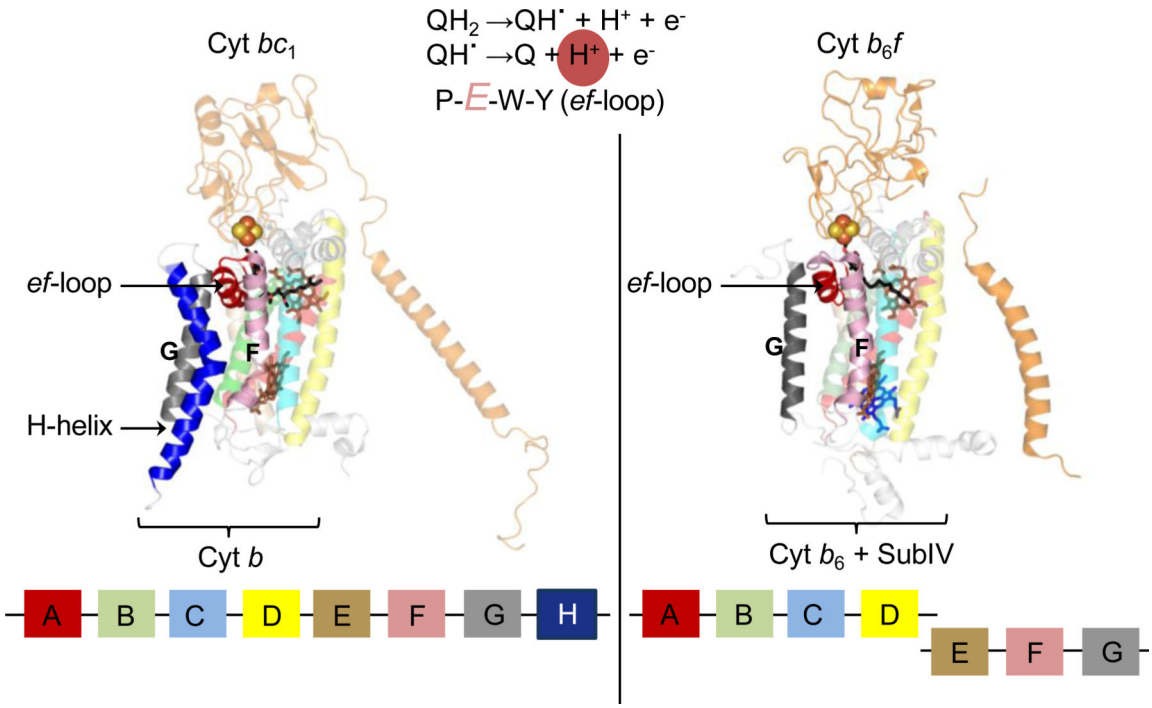

Figure 6. Organization of the Q_p-site in cyochrome bc complexes

The *ef*-loop bears the conserved PEWY sequence, whose Glu residue is involved in the second deprotonation reaction (highlighted in reaction sequence) of the substrate within the Q_p-site. **Left panel:** In the cyt bc_1 complex (PDB ID 3CX5), the *ef*-loop is inserted between the F and G transmembrane helices of the 8 helix cyt *b* polypeptide (shown in block diagram at the bottom). The space between the F and G TMH is stabilized by the H TMH of cyt *b*. **Right panel:** In the cyt b_6f complex (PDB ID 2E74), the 'H' TMH is absent from the subIV polypeptide (shown as block diagram). This niche is occupied by a lipid and a chlorophyll-*a* molecule.

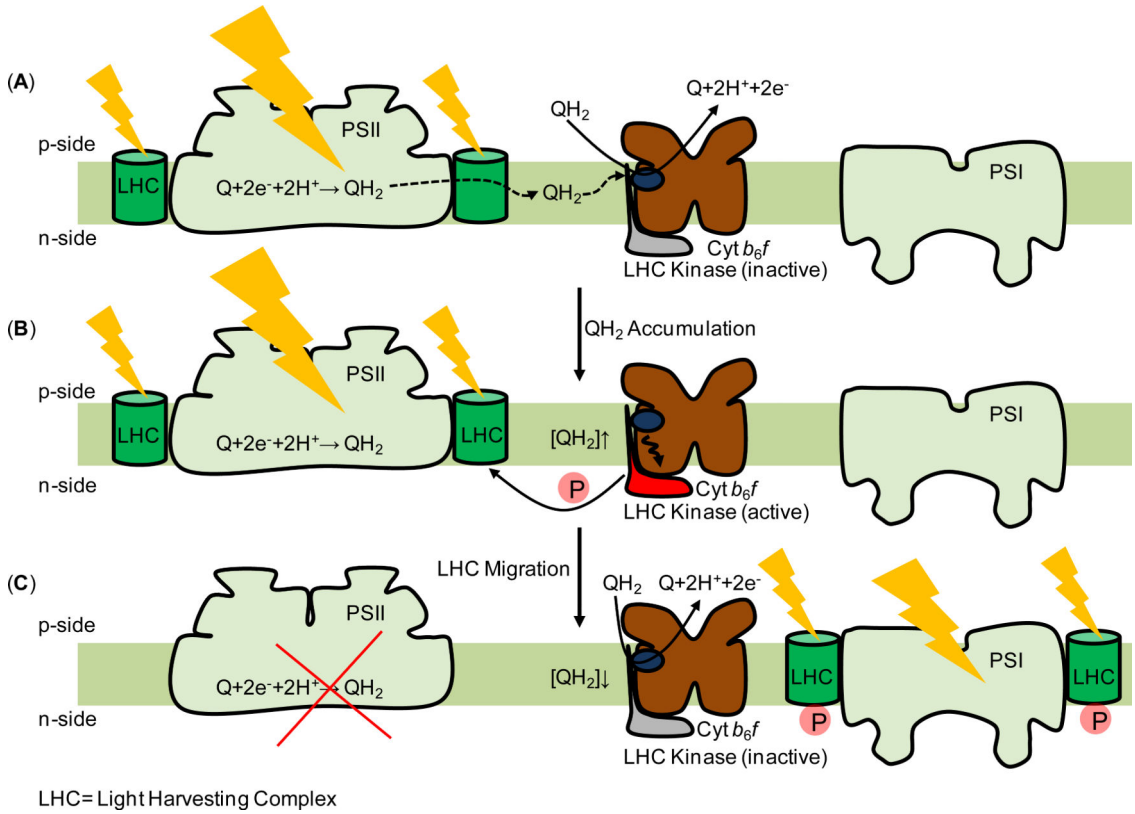

Figure 7. Photosynthetic state transitions

(**A**) The photosystem II (PSII) reaction center complex utilizes light energy harvested by accessory light harvesting complex II (LHC) molecules to reduce plastoquinone (PQ) to plastoquinol (PQH_2). PQH_2 undergoes diffusion to the Q_p-site (blue circle) of the cyt b_6f complex (brown cartoon), where it undergoes oxidation. (**B**) Slow PQH_2 oxidation by cyt b_6f causes PQH_2 accumulation in the thylakoid membrane, which activates the LHCII kinase (shown in red). (**C**) In the phosphorylated state, LHC molecules migrate to photosystem I (PSI), thereby reducing the efficiency of PQ reduction by PSII. As PQH_2 consumption by cyt b_6f is not affected, a redox balance is restored in the quinone pool, which inactivates the LHCII kinase (shown in gray).

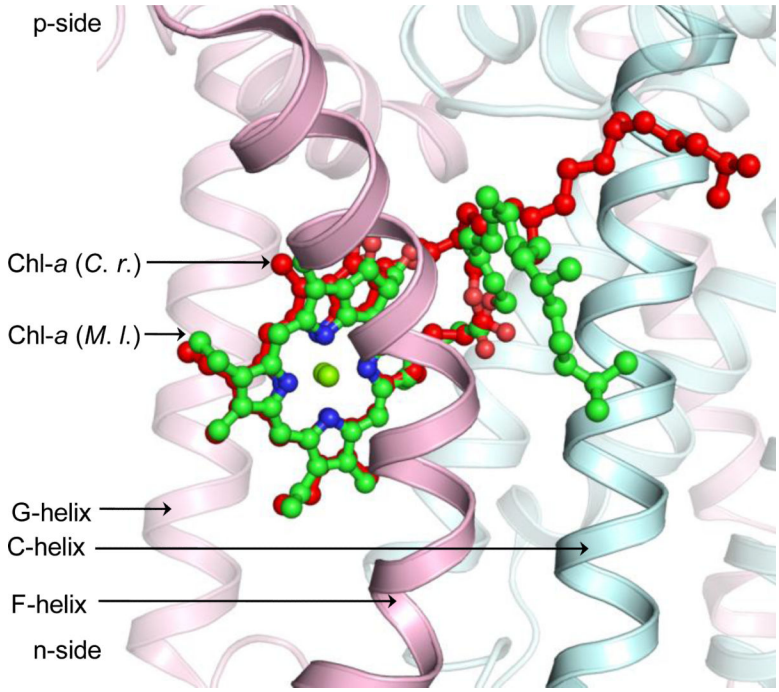

Figure 8. Alternate conformations of the chl-a phytyl-tail in cyt b_6f

The chl-*a* chlorin-ring is inserted between the F and G TMH of subIV (light pink) while the tail is inserted between the F TMH and the C TMH of cyt b_6 (pale cyan). In the crystal structure of cyt b_6f (PDB ID 2E74) from the cyanobacterium *M. laminosus*, the chl-*a* phytyl-tail (green) is wrapped around the F TMH while in the structure obtained from *C. reinhardtii*, the chl-*a* phytyl-tail (red) is located proximal to the C TMH.

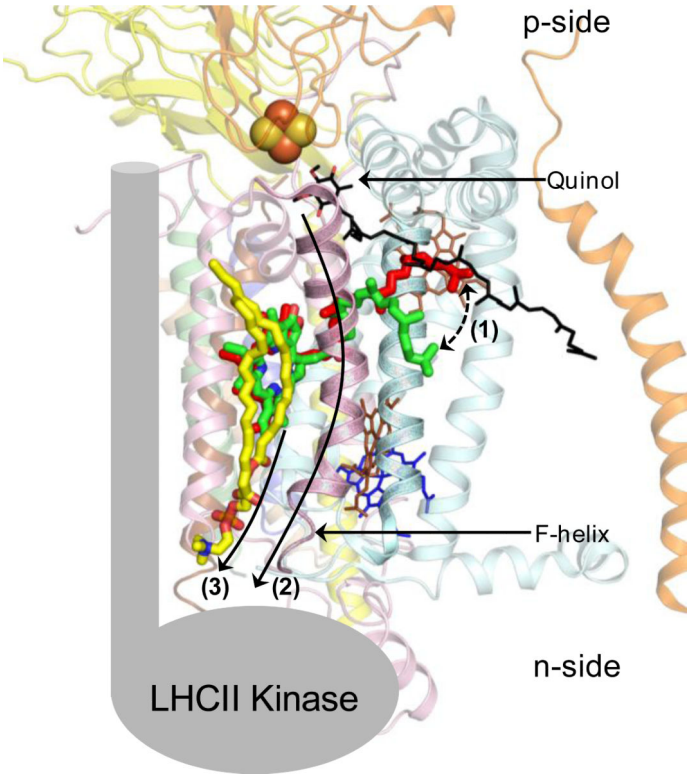

Figure 9. Proposed mechanism of chl-a mediated signal transduction in the cyt b_6f complex (PDB ID 2E74) for activation of photosynthetic state transitions

(**Step 1**) Binding of the natural substrate plastoquinol (black/red sticks) within the Q_p-site displaces the chl-*a* phytyl-tail (displacement shown as broken line with arrows) due to interaction with the long isoprenoid tail of the palstoquinol molecule. The displacement event generates a signal that is transduced to the n-side of the complex either (**Step 2**) via the F TMH or (**Step 3**) through a combination of the F TMH and the n-side lipid (yellow) present between the F and G TMH. The LHCII kinase is shown (gray) in cartoon format.

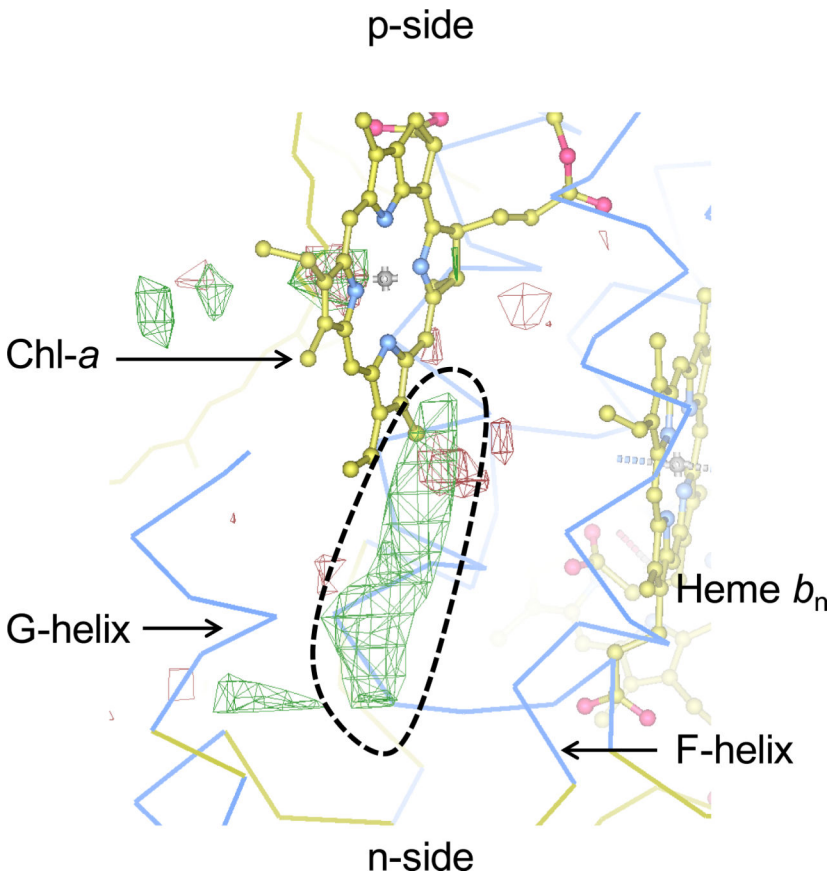

Figure 10. Potential lipid binding site in cyt b_6f complex of C. reinhardtii

The cyt b_6f structure (PDB ID 1Q90) was obtained in the presence of native lipids. Residual electron density is shown as green mesh (highlighted by broken black line) between the Fo-Fc map (3.0 σ). The electron density corresponds to the n-side lipid in the cyanbacterial cyt b_6f complexes from *M. laminosus* (PDB ID 2E74) and *Nostoc* PCC 7120 (PDB ID 2ZT9). The electron density map was obtained from the Electron Density Server [96].

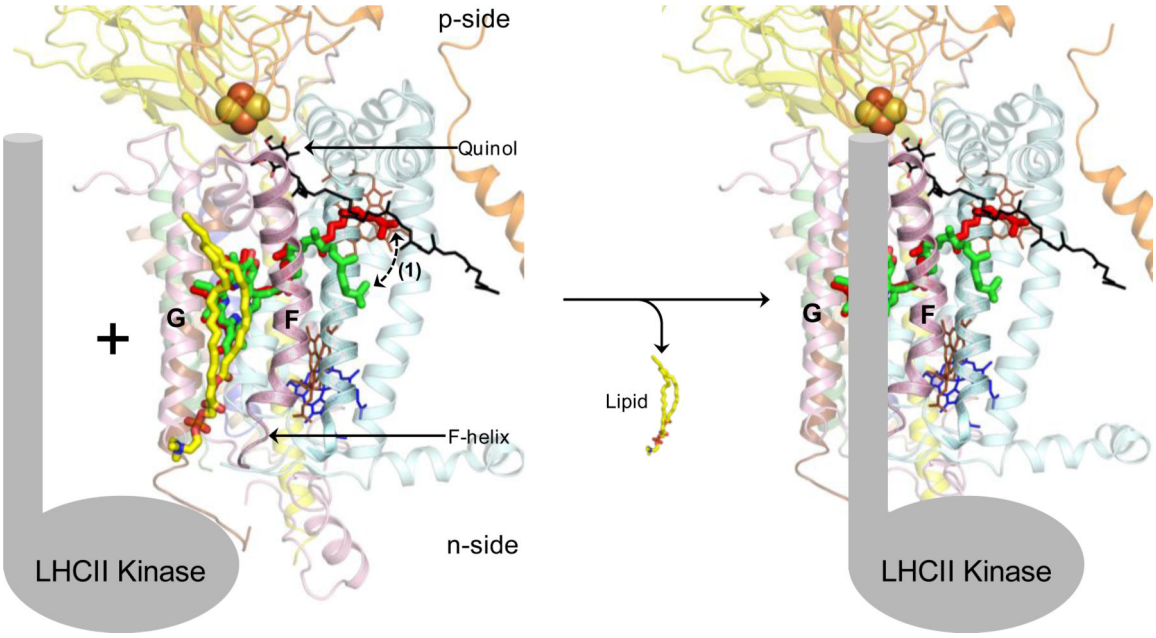

Figure 11. The lipidic mechanism of cyt b_6f-LHCII kinase super-complex formation

It is proposed that the lipid DOPC (yellow/red/blue sticks) is bound weakly in the niche formed between the F and G TMH, which represents the LHCII kinase (shown as cartoon. gray) binding site. Recruitment of the LHCII kinase to the cyt b_6f complex and binding results in the replacement of the lipid from the inter-helix niche.

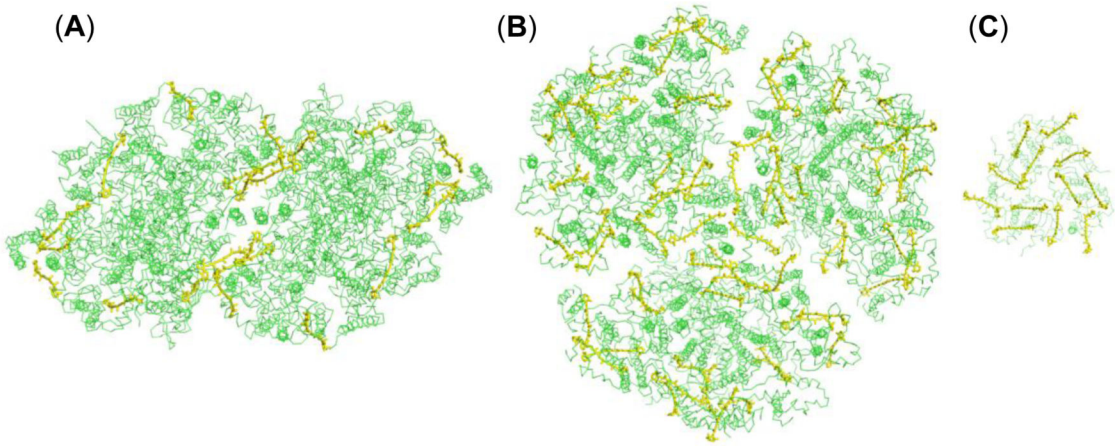

Figure 12. Arrangement of β–carotene in the major photosynthetic integral membrane protein complexes (A) photosystem II (PDB ID 3ARC), (B) photosystem I (1JB0) and light harvesting complex II (PDB ID 2BHW)

The β–car molecules are shown as yellow sticks while the polypeptides are represented as thin green ribbons. The β-car molecules are located on the periphery of the complexes, providing potential interaction sites for the chl-*a* of cyt b_6f. All three complexes are viewed along the normal to the membrane plane. For simplicity, other prosthetic groups have been omitted.

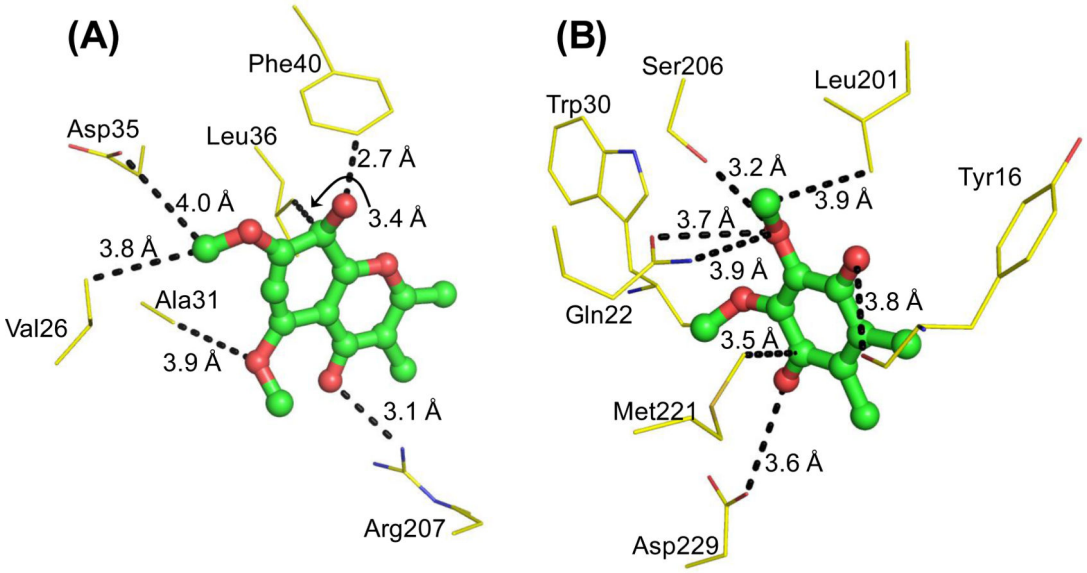

Figure 13. Binding of ligands to the Q_n-site of cyt bc complexes and the role of the protein environment in selectivity

(**A**) In the cyt b_6f structure (PDB ID 2E76) obtained from the cyanobacterium *M. laminosus*, the majority of the interactions to the quinone analog inhibitor TDS (green/red ball and stick model) are contributed through non-specific Van der Waals interaction. (**B**) On the other hand, binding of the natural ligand ubiquinone-6 (green/red ball and stick model) to the cyt bc_1 complex (PDB ID 1KB9) Q_n-site is mediated by polar interactions. For simplicity, the hydrophobic tails of TDS and ubiquinone-6 have been omitted.

Table 1

Subunits of the cytb_6f complex (*M. l., M.laminosus, C. r., C. reinhardtii*) [39]

Subunit	**MW (kDa)**	**MW (kDa)**	**pI**	**pI**	E_{m7} **(mV)**
	M. l.	***C. r.***	***M. l.***	***C. r.***	
Cyt *f* (1 heme)	32.273	31.249	6.7	8.3	+350-380
Cyt b_6 (3 hemes)	24.712	24.165	9.0	8.8	(−50, bn); −50 to −150, b_p; +100, C_n
ISP [2Fe–2S]	19.295	18.333	6.8	5.8	+300 - 320
SubIV	17.528	17.295	8.1	6.6	--
PetG	4.058	3.984	4.5	4.4	--
PetM	3.841	4.036	10.4	4.3	--
PetL	3.530	3.436	10.2	9.5	--
PetN	3.304	3.282	5.7	6.0	--